Title: Resolving spatial complexities of hybridization in the context of the gray zone of speciation in North American ratsnakes (*Pantherophis obsoletus* complex)

Frank T. Burbrink[1*]

Marcelo Gehara[1,2]

Edward A. Myers[1,3]

[1]Department of Herpetology, The American Museum of Natural History, Central Park West and 79th Street, New York, NY 10024 USA

[2]Department of Biological Sciences, Rutgers University Newark, 195 University Ave, Newark, NJ 07102

[3]Department of Vertebrate Zoology, National Museum of Natural History, Smithsonian Institution, Washington, DC, USA

***Corresponding author** – fburbrink@amnh.org

Abstract:

Estimating species divergence with gene flow has been crucial for characterizing the gray zone of speciation, which is the period of time where lineages have diverged but have not yet achieved strict reproductive isolation. However, estimates of divergence times and gene flow often ignores spatial information, for example the formation and shape of hybrid zones. Using population genomic data from the eastern ratsnake complex (*Pantherophis obsoletus*), we infer phylogeographic groups, gene flow, changes in demography, the timing of divergence, and hybrid zone widths. We examine the spatial context of diversification by linking migration and timing of divergence to the size, shape, and types of hybridization (e.g., F1, backcrosses) in hybrid zones. Rates of migration between lineages are associated with the width and shape of hybrid zones. Timing of divergence is not related to migration rate across species pairs and is therefore a poor proxy for inferring position in the gray zone. Artificial neural network approaches are applied to understand how landscape features and past climate have influenced population genetic structure among these lineages prior to hybridization. The Mississippi River produced the deepest divergence in this complex, whereas Pleistocene climate and elevation secondarily structured lineages.

Key Words: Eastern Nearctic, migration, isolation, neural networks, reproductive isolation, cline, hybrid zone

Wide-ranging species complexes that cross numerous biogeographic barriers provide opportunities to better understand how changing landscapes affects diversification, gene flow, demography, and the formation of hybrid zones. Lineages within species complexes ranging

52 across heterogeneous landscapes are likely at different stages of the speciation process reflecting
53 how specific environmental and biogeographic barriers have uniquely altered changes in gene
54 flow and other demographic processes in a particular complex (Myers et al. 2020). Even at the
55 same barrier within related groups of organisms, the timing of divergence and degree of gene
56 flow can be species specific and dependent on when they encountered the barrier (Riddle 2016;
57 Myers et al. 2019). Alternatively, generalist species not as constrained to specific habitats may
58 not show a correlation between genetic variation and landscape features (Joseph and Wilke 2007;
59 Makowsky et al. 2009; Lourenço et al. 2017).

60 Lineage divergence can be placed in the context of the gray zone of speciation, which
61 defines the range of time where speciation proceeds from early population differentiation with
62 unfettered gene flow to nearly reproductive isolation defined by low rates of gene flow (de
63 Queiroz, 2007; Hewitt, 2008; Jackson et al., 2016; Roux et al., 2016). The ability to delimit
64 species therefore may be correlated with their position in the gray zone, which has previously
65 been assessed by relating measures of genetic isolation and migration (the genealogical
66 divergence index; GDI) with species-delimitation probabilities (Jackson et al. 2016; Leaché et al.
67 2019). Moreover, given a model of speciation that proceeds by Dobzhansky-Muller
68 incompatibilities and genetic drift alone, the degree of gene flow might be predicted by the age
69 of lineage formation relative to population size and thus position within the gray zone (Orr 1995;
70 Gavrilets 2004; Singhal and Moritz 2013). Clearly some bias exists here; enhanced gene flow
71 between the youngest divergences may never proceed to the later stages in the gray zone as they
72 may rapidly collapse into a single lineage (Garrick et al. 2019), such as in the case where
73 physical barriers to gene flow disappear. On the other hand, strong selection may prevent young
74 lineages from exchanging alleles at particular loci, shortening the time in the gray zone (Mayr

75 1963; Barton 2010; Feder et al. 2012; Roux et al. 2016; Edwards et al. 2020). Therefore, finding
76 a threshold that can determine if two species are unique given only generations since divergence
77 may fail in cases where rates of gene flow between lineages drastically change over time and
78 space (Gourbière and Mallet 2010; Nosil et al. 2017).

79 Conceptualizing the gray zone without a spatial demographic component therefore may
80 be inadequate for understanding speciation and delimiting species. Isolation-migration models
81 (Hey and Nielsen 2004; Hey 2010) are coalescent estimators of historical processes and can
82 assess gene flow throughout time, reflecting position in the gray zone of speciation. These
83 models, however, lack any spatial component necessary to understand the underlying geographic
84 and environmental processes influencing migration. Studies of hybrid zones on the other hand
85 can clarify the location of migration and rates of contemporary gene flow, provided selection
86 does not eliminate F1 hybrids or backcrossing. If species pairs rapidly adapt to unique habitats
87 across their distribution, then age of divergence and degree of gene flow may be unrelated
88 relative to neutral processes when compared across taxa (Nosil and Crespi 2006; Agrawal et al.
89 2011; Nosil 2012; Karrenberg et al. 2019). Therefore, divergence over landscape can show how
90 selection at a barrier can be discordant from the timing of origin of the lineages (Barton and
91 Hewitt 1985; Harrison 1993; Jiggins and Mallet 2000; Gay et al. 2008; Seehausen et al. 2014;
92 Stankowski et al. 2017). Combining spatial information with genetic data will better help
93 understand how genetic variation is structured by geographic distance, environment, and the
94 presence of hybrid zones. This should provide a clearer understanding of why lineages maintain
95 particular rates of gene flow along a biogeographic barrier that has resulted in a hybrid zone.
96 Moreover, investigating gene flow in space determines if lineages were generated via isolation

97 and migration or are simply artificially partitioned groups with continuous gene flow over the
98 landscape defined by IBD (Wright 1943; Frantz et al. 2010; Bradburd et al. 2018).
99 To understand the factors shaping reproductive isolation in a species complex, we ask
100 whether divergence time predicts rates of gene flow or cline width across space in eastern
101 ratsnakes (*Pantherophis obsoletus* complex). This complex is a wide-ranging group of four
102 species found throughout the forested regions of the Eastern Nearctic and nearby Chihuahuan
103 Desert that have diverged at three unique biogeographic barriers. The primary divergence in this
104 complex occurred at the Mississippi River, which has consistently been identified as one of the
105 main biogeographic barriers in the ENA (Robison 1986; Burbrink et al. 2000; Soltis et al. 2006;
106 Brandley et al. 2010; Zellmer et al. 2012; Myers et al. 2020). Further east, the Appalachian
107 Mountains and Apalachicola/Chattahoochee River System (AARS) have noted barrier effects in
108 other organisms and likely contributed to the divergence between *P. alleghaniensis* and *P.*
109 *spiloides* (Walker and Avise 1998; Burbrink et al. 2000; Soltis et al. 2006). West of the
110 Mississippi River, divergences occurred at the transition between temperate forests to the rocky
111 areas on the western edge of the Edwards Plateau into the Chihuahuan Desert and isolated the
112 species *P. obsoletus* and *P. bairdi* (Fig.1; Lawson and Lieb 1990; Burbrink et al. 2000; Burbrink
113 2001). Since the Pliocene, the ENA has experienced numerous climate change events associated
114 with glacial cycles that forced species into refugia and compressed populations; upon climate
115 amelioration populations expanded into formerly glaciated areas (Hewitt 2000; Bintanja and van
116 de Wal 2008; Burbrink et al. 2016). Using dense population sampling and genomic-scale data,
117 we combine isolation-migration estimates with spatial information to understand species
118 divergence in the context of geographic distance, contemporary and historical environments, and
119 biogeographic boundaries. We also examine how migration rates and divergence dates relate to

120 the width and types of hybrids (F1, backcrosses) in these hybrid zones at biogeographic
121 boundaries. We also investigate demographic changes through time to understand if population
122 expansion occurs among all lineages as predicted given glacial cycling. Addressing these
123 questions provides an integrated view of phylogeographic history over a physically and
124 historically complex landscape and yields a clearer understanding of speciation processes and
125 delimitation in the gray zone.
126
127
128 **Methods**
129
130 *Dataset*
131 We sampled 288 individuals liberally covering the range of all species within the
132 *Pantherophis obsoletus* complex (Fig.1; Dryad XXX). DNA was extracted from all samples
133 using Qiagen DNeasy Blood & Tissue Kits and samples were screened for quality using broad-
134 range Qubit Assays. We used services from RAPiD Genomics (https://www.rapid-
135 genomics.com/services/) to generate 5472 baits and to sequence 5060 conserved elements
136 (UCEs) loci following the protocols from (Faircloth et al. 2012) and (Sun et al. 2014). These
137 markers have been used to address phylogeographic/population genetic and deeper phylogenetic
138 questions (Branstetter and Longino 2019; Younger et al. 2019). We mapped UCE reads to a
139 Chromium 10x *Pantherophis spiloides* genome (in prep), removed loci containing >50% missing
140 samples, and removed individual specimens missing >30% of all alignments (details on the
141 assembly of UCE loci are available in Supporting Information Material 1). We produced both
142 phased locus datasets, used in PHRAPL and PipeMaster, and single SNPs/locus for all other

143 analyses, furthermore we filtered the unlinked SNP dataset to remove alleles with a minor allele
144 frequency <0.1 and used these data for population structuring analyses.
145
146 *Geographic groupings*
147 We estimated population structure by comparing Discriminant Analysis of Principal
148 Components (DAPC; Jombart et al., 2010) in adegenet v2.1.2 (Jombart 2008). We compared this
149 to estimated effective migration surfaces (EEMS v; Petkova et al., 2016), which models effective
150 migration rates over geography to represent regions where migration is low in cases where
151 genetic dissimilarity increases rapidly, thus providing a uniquely distinct view of the location of
152 population clusters relative to biogeographic barriers as compared to DAPC (details on these
153 population grouping methods and other methods for assessing structure are available in
154 Supporting Information Material 1). We also examined fixation indices (F_{ST}) estimated from Nei
155 (1973) in adegenet v2.1.2 (Jombart 2008) across all loci comparing spatially adjacent lineage
156 pairs from DAPC .
157
158 *Isolation, migration, and historical demography*
159 We generated a coalescent-based species tree with SNAPP v1.3.0 (Bryant et al. 2012) to
160 understand relationships among the four taxa identified from clustering analyses and test species
161 delimitation. Because generating a tree in SNAPP using all individuals was computationally
162 intractable, we used four individuals per taxon that were sampled from different regions of the
163 taxon's distribution. We estimated SNAPP trees using BEAST v2.5.2 (Bouckaert et al. 2014;
164 details on parameter setting for SNAPP are available in Supporting Information Material 1). We
165 assessed four alternative species delimitation models including four taxa, three taxa (collapsing

166 *P. bairdi/P. obsoletus* or *P. alleghaniensis/P. spiloides*), and two taxa (collapsing *P. bairdi/P.*
167 *obsoletus* and *P.alleghaniensis/P. spiloides)*.

168 Using the four inferred lineages, we examined which models best described the origins of
169 these groups given divergence time, historical demographic change, and migration between
170 spatially adjacent taxa. We tested 2,300 candidate isolation-migration models including all
171 possible topologies with or without migration between all spatially adjacent pairs using the
172 program PHRAPL (Jackson et al. 2016) implemented in R. To further test that four genetic
173 lineages exist, we ran pairwise comparisons between the best selected model and models of three
174 populations where sister species were collapsed into a single entity; four *Pantherophis* species
175 against one model where *P. obsoletus* and *P. bairdi* were collapsed, and another where *P.*
176 *spiloides* and *P. alleghaniensis* were collapsed (details on PHRAPL runs are available in
177 Supporting Information Material 1).

178 To estimate gene flow, timing of divergence, and demographic change, we used
179 PipeMaster (Gehara et al., 2017; Gehara et al. in review) to simulate genetic data and perform
180 approximate Bayesian computation (ABC) and supervised machine-learning. Here we used the
181 best model selected in the PHRAPL analysis as a template (same topology and migration
182 parameters) to generate three competing models: (i) an isolation migration model with constant
183 population size for each lineage and constant migration, (ii) demographic change along each
184 lineage and constant migration through time and demographic change, and (iii) population size
185 change with migration occurring after the Last Glacial Maximum. We simulated 100,000 data
186 sets of 54 summary statistics and performed ABC rejection with 0.01 tolerance level to select the
187 best of these three models (Table S1). We then took the selected model and performed rejection

188 using a 0.1 tolerance level with a neural network regression using a single layer and 20 nodes to
189 estimate the model parameters.
190
191 *Spatial population genetics*
192 We used artificial neural networks (ANN; Lek and Guégan 1999; Legendre and Fortin
193 2010; Legendre et al. 2011) to understand how contemporary and historical aspects of the
194 landscape and climate generated genetic diversity. We first compared niche models of current
195 climates between adjacent species pairs to determine if contemporary niches were significantly
196 different prior to using these variables for understanding their effects on genetic structure (see
197 Supporting Information Material 1 for details). We then used Nei's distance (Nei, 1972) to
198 estimate genetic distance among all individuals in the R package adegenet. For predictor
199 variables, we used 1) geographic distances measured as pairwise great-circle distances among all
200 points to account for isolation-by-distance using the R package fossil (Vavrek 2020), 2) binary
201 categorization of isolation east and west of the Mississippi River, 3) elevation, and 4) bioclimatic
202 variables at 2.5 mins representing current climate, Last Glacial Maximum (21kya), Last
203 Interglacial (130 kya), Pleistocene Marine Isotope Stage 19 (787 kya) and Mid-Pliocene
204 Warming (3.2 Ma) all obtained from the PaleoClim database (Brown et al. 2018). For the
205 bioclimatic data and elevation, we extracted parameter values given the latitude and longitude for
206 each individual sample. To reduce dimensionality of the bioclimatic variables, we transformed
207 the former using principal components analyses using the R package raster (Hijmans et al. 2014).
208 Spatial distances were transformed using principal coordinates analyses in the R package ape
209 (Paradis and Schliep 2019). For principal coordinate/component analyses we retained axes that
210 account for >95% of variance.

211 We used regression-based ANN to determine which variables predict genetic distances
212 and rank those with the highest model importance. Machine learning methods can infer non-
213 linear interactions among many predictor variables, regardless of the distribution or variable type
214 and can generate a range of models of varying complexity (Lek et al. 1996; Zhang 2010;
215 Libbrecht and Noble 2015; Sheehan et al. 2016). To conduct the ANN regressions we used the R
216 package *caret* (Kuhn 2008) and partitioned the data into the standard 70% training and 30% test
217 sets (Lek et al. 1996; Zhang 2010; Burbrink et al. 2020). This analysis was run using 1,000
218 maximum iterations to ensure convergence. We resampled the data using the default 25 bootstrap
219 replicates to reach convergence over the following parameters: weight decay, root mean squared
220 error, r^2, and mean absolute error. We assessed the power of these models by recomposing the
221 test and training sets 100 times and compared three test statistics (root mean squared error, r^2,
222 and mean absolute error) to those from randomized response variables for each of these 100 re-
223 estimated models. We ranked the most important variables over these replicates after accounting
224 for multicollinearity among variable affects using the R package Rnalytica (see Supporting
225 Information Material 1). We also compared results from our ANN analysis to those using
226 redundancy analyses (RDA, see Supporting Information Material 1 for details).
227
228 *Hybrid-zone dynamics*
229 To understand if the composition and width of hybrid-zones differed among adjacent
230 lineages we first estimated the composition of individuals and their locations (parentals, F1s,
231 backcrosses). We first used *snapclust* (Beugin et al. 2018) in adegenet to assign pure parentals
232 (P1 and P2), backcrosses and F1s between the following spatially adjacent pairs of taxa, herein
233 referred to by geographic area: 1) eastern (*P. allegahniensis/P. spiloides)*, 2) central (*P.*

234 *spiloides/P. obsoletus),* and 3) western (*P. obsoletus/P. bairdi)*. This method maximizes the
235 likelihood of two fixed panmictic populations using a geometric approach with an expectation-
236 maximization algorithm. We estimated group membership first using the "k-means" option in the
237 function. To check the probability that *snapclust* identified hybrids correctly with these data, we
238 isolated pure parental individuals (membership >0.95), used the *hybridize* function to generate
239 the same number of hybrids and parentals and then determined the probability that *snapclust*
240 finds the correct number of hybrids and parentals.

241 We then fit clines in the program HZAR v.2-9 (Derryberry et al. 2014) for the same
242 species pairs using individual genetic assignments from DAPC to determine if cline widths differ
243 among groups. We compared these to ancestry alternatively estimated in *snaplcust* (see
244 Supporting Information Material 1 for details). Using the Gaussian cline model, we estimated the
245 center and width of the cline and determined if these sigmoidal distributions have significant tails
246 by fitting the following models: 1) no tails, 2) right tail only, 3) left tail only, 4) mirrored tails,
247 and 5) both tails estimated independently (see Derryberry et al. 2014). We fit these models to our
248 data using AICc and ran the MCMC chains for $5x10^6$ generations, thinned by $5x10^3$ generations,
249 and estimated stationarity using ESS >200 in the R package CODA (Plummer et al. 2006). We
250 note that making transects through multiple locations along each hybrid zone would better define
251 the width throughout the length of the cline, though this was not possible here for all clines.

252 Using equations from Barton and Gale (1993) and applied in Bailey et al. (2015) we
253 addressed selection against hybridization for each cline. Using estimates of maximum lifetime
254 dispersal (σ) for ratsnakes, here 0.937-4.3 km (Weatherhead and Blouin-Demers pers comm.),
255 we predict the width of the cline under neutrality over a range of generation times (T) since the
256 origin of each sister pair and group using the equation: $w = 2.51\sigma\sqrt{T}$. We also predict selection

257 at the center of the cline, also using σ and estimates of cline width (*w*) from HZAR using the
258 equation:
259 $S = \left(\frac{2\sigma}{w}\right)^2$. We estimate these given the range of dispersal estimates and estimates for the widths
260 of clines.
261
262 All scripts, genetic, and spatial data are available on Dryad XX.
263
264
265 **Results**
266 *Data and population genetic structure*
267 After filtering loci for presence in 70% or more individuals, we generated 2,491 UCE
268 loci. For all downstream analyses we randomly sampled one SNP per locus yielding a total of
269 846 SNPs for 238 individuals for an average of 13.96% missing data.
270 Both EEMS and DAPC find population structure that generally matched the geographic
271 ranges of *P. alleghaniensis*, *P. spiloides, P. obsoletus*, and *P. bairdi* (Fig. 1 and Fig. S1;
272 Burbrink, 2001). All three EEMS generated similar acceptance proportions for all proposal types
273 (12-51%). Total DAPC assignment probabilities without apriori species groupings were 0.975
274 (*P. bairdi* = 1.0, *P. obsoletus* = 0.96; *P. spiloides* = 1.0, and *P. alleghaniensis* = 0.97). Similarly,
275 all three EEMS runs suggest low migration at the MR and the area separating the *P. bairdi* and
276 *P. obsoletus* in west Texas. East of the MR, estimated low migration occurred near the
277 Appalachian Mountains, though this area is a complex mixture of isolation and gene flow (Fig.
278 1).

279 These estimates of population structure all showed *P. alleghaniensis* as occurring mostly
280 in the Florida Peninsula and north along the east coast to Virginia/Delaware (not as far north as
281 in Burbrink 2001), *P. spiloides* is found from western Florida to the Mississippi River up through
282 the Midwest and east to the northeastern US, *P. obsoletus* is found west of the Mississippi River
283 in the forested regions of the Midwest, and *P. bairdi* is distributed in the Chihuahuan Desert of
284 west Texas (Figs.1-2).
285
286 *Isolation-migration processes*
287 Our SNAPP analyses produced a phylogeny with a root separating the taxa east and west
288 of the Mississippi River and then a sister relationship between *P. bairdi* and *P. obsoletus* and
289 then *P. spiloides* and *P. alleghaniensis* (Fig. 2), consistent with Burbrink et al., (2000). Bayes
290 factors (BF) showed the four-taxon model as decisively superior to the three-taxon (BF =35.40)
291 and two-taxon model (BF=2022.46).
292 Using those four lineages we filtered models of divergence using PHRAPL. Models with
293 all four taxa, incorporating migration between spatially adjacent lineages was preferred with the
294 same topology as found using SNAPP. ΔAIC between the best ranked model and next model was
295 > 20, suggesting high confidence in model selection (Table S2).
296 The demographic model estimated from PipeMaster that incorporated historical
297 population size change and constant migration (IMD) best fit the data (posterior probability 1.0;
298 see PCA plots in Fig. S2; Figs. 2 & 3). Median migration rates were highest between eastern
299 groups (*P. alleghaniensis* to *P. spiloides* = 2.79 and *P. spiloides* to *P. alleghaniensis* = 3.79
300 individuals/generation), lower in the central groups across the Mississippi River (*P. spiloides* to
301 *P. obsoletus* = 1.96 and *P. obsoletus* to *P. spiloides* = 1.28 individuals/generation), and lowest in

302 western groups (*P. bairdi* to *P. obsoletus*= 0.55 and *P. obsoletus* to *P. bairdi* = 0.65
303 individuals/generations; Table 1). Divergence occurred earliest in the central lineages at the
304 Mississippi River at 1.08 My (95% CI =0.553 to 1.674 My), then the eastern lineages at 0.650
305 My (95%CI = 0.225 to 0.983 My) and western lineages at 0.367 My (95% CI 0.367 to 0.875 My;
306 Table 1). Divergence dates and average rates of migration were poorly correlated (ρ=0.264,
307 P=0.83, n=3). For all taxa we inferred population expansion from ancestral N_e sizes ranging from
308 5,200 to 5,600 to modern sizes at 138,000 to 281,000. The posterior distributions for all
309 parameters were different from the uniform priors, though wide distributions of several
310 parameters suggested some uncertainty in estimates (Fig. 3).
311
312 *Spatial population genetics and hybrid zones*
313 We used ANN to determine what features of the landscape and environmental layers
314 through time best predict genetic structure (Fig.4). Contemporary niches between taxa were
315 significantly different for all taxa (see Supporting Information Material 1 for details, Fig. S3).
316 Estimates of accuracy using ANN were high (>90%) for all comparisons. Most genetic structure
317 can be predicted by the Mississippi River showing 100% variable importance (Table S3).
318 Distance also played a role in structuring these data (although they were partialed out in RDA
319 analyses yielding similar conclusions regarding other landscape variables, see Supporting
320 Information Material 1). For those lineages east of the Mississippi River, population structure
321 was predicted by climate at the Last Glacial Maxima and elevation (variable importance=100).
322 For those lineages west of the Mississippi River, climate during Pleistocene Marine Isotope
323 Stage 19 and elevation structured these lineages (variable importance = 100).

324 Using *snapclust,* we showed that the number of hybrids of all types decreases with
325 species pair comparisons from east to west (Fig. 5). The parentals, hybrids and backcrosses were
326 predicted with a mean accuracy of 0.99 in simulations. All hybrid types were spatially oriented
327 between parental types where the number of hybrids and backcrosses between the eastern groups
328 approached the number of parental individuals (49%), for the central groups the hybrids and
329 backcrosses to parental ratio was 5.9%, and for the western groups there were no hybrids
330 detected (Fig. 5). It is important to note, however, that sampling was more concentrated between
331 *P. alleghaniensis/P. spiloides* compared to the other pairs.
332 For the eastern lineages, HZAR showed strong support for a right-tailed model
333 (ΔAIC_{DAPC} =-31.96 – -107.42), whereas central lineages at the Mississippi River (ΔAIC_{DAPC} = -
334 4.26 – -8.869) and western lineages at the Chihuahuan Desert and Edward's Plateau (ΔAIC_{DAPC} =
335 -5.51 – -221.35) both supported a no-tails model (Fig. 6; Table S4 & S5). However, estimating
336 tailed models for the latter two comparisons may have required more samples than were
337 available. The width of clines decreased from the eastern lineages (width=126 km, 1st and 3rd
338 quartiles 114-138 km, tail length =53 km, 1st and 3rd quartiles 44-61 km), to central (width = 98
339 km, 1st and 3rd quartile 89-107 km), to the western lineages (width = 8 km, 1st and 3rd quartile =4-
340 15 km; Table 1). Sharply declining hybrid zones characterized the central and western lineages,
341 whereas the cline for eastern lineages showed a long right tail extending north.
342 Hybrid zone widths under neutrality should be larger than the actual widths given that
343 migration between sister pairs likely occurred prior to the LGM (Fig. S4). Contact time for each
344 of these pairs to approach the same actual width sizes all occurred within the Holocene: 516-
345 10,785 ybp (eastern lineages*),* 261-5424 ybp (central lineages) and 3-27 ybp (western lineages).
346 We also showed that selection against hybrids at the center of hybrid zones ranged from a

347 median of 0.3 % (0.02-0.6%) for eastern, 0.5% (0.03 to 1%) for central, and 79% (1.5-100%) for
348 western lineages.
349 When using a single SNP per locus we showed that 30% of loci from central lineages,
350 10.9% of loci for western lineages, and only 1.9% of loci for eastern lineages attained an F_{st}
351 >0.35. Given demographic histories between comparisons, this threshold for F_{st} is generally
352 considered extreme population disconnection beyond which advantageous loci will be exchanged
353 between populations (Wright 1978; Frankham et al. 2010).
354
355 **Discussion**
356 *Grey Zone Dynamics*
357 To understand the factors shaping reproductive isolation in a young species complex, we
358 ask whether divergence time predicts rates of gene flow or cline width across space in eastern
359 ratsnakes. This species complex is composed of four divergent lineages, with *P. alleghaniensis*
360 and *P. spiloides* meeting in the southeastern US at the intersection of subtropical and temperate
361 areas, *P. spiloides* and *P. obsoletus* separated at the Mississippi River, and *P. obsoletus* and *P.*
362 *bairdi* meeting at the connection on the forested and rocky habitats on the western edge of the
363 Edwards Plateau. All three spatially adjacent pairs of taxa show variable migration each having
364 unique cline shapes. The western lineages (*P. obsoletus*, *P. bairdi*) show very low migration
365 rates, a cline equivalent to only 0.35% of the parental range, fixation (F_{st} > 0.35) in 10.9% of
366 loci, and likely selection against hybrids. This is in comparison with central lineages (*P.*
367 *obsoletus, P. spiloides*) showing more migration, a cline occupying 5% of the parental ranges,
368 but with 35% of loci showing fixation, and possibly lower selection. Finally, eastern lineages (*P.*
369 *alleghanienis, P. spiloides*) have incomplete reproductive isolation (showing numerous F1 and

370 backcrosses) with only 1.9% of loci showing fixation, and high migration rates with a clinal tail
371 (Figs. 3 & 6). Where reproductive isolation occurs given low numbers of migrants/generation,
372 there is increased fixation among loci and steeper clines occur. The inverse is also true; when
373 reproductive isolation is incomplete, higher rates of gene flow less fixation of loci, and variable
374 cline widths occur. Importantly, however, reproductive isolation, gene flow estimates, and hybrid
375 clines show no association with timing of divergence.

376 Hybrid zone dynamics help to understand the interactions between pairs of taxa as
377 characteristics of the hybrid zone reveal whether there is selection against hybrids (tension
378 zones), selection for hybrids (bounded superiority), or ecological gradients with reduced fitness.
379 They also reveal whether selection is endogenous (genomic) or exogenous (environmental;
380 Barton and Hewitt 1985; Barton and Gale 1993). Our models indicate that migration at the
381 Mississippi River and in the eastern lineages occurred through the Pleistocene suggesting some
382 form of a hybrid zone existed through major climate change cycles. Given this age and assuming
383 selective neutrality, we demonstrate that these hybrid zones should be much larger, in most cases
384 exceeding the ranges of parental taxa (Fig. S4). The widths of the current hybrid zones are
385 maintained over time, preserving the historical and geographic identity of the parental taxa.
386 While there is some selection against hybrids as estimated from hybrid zone width and dispersal,
387 depending on species-pair comparison, it is possible that other factors may be constraining these
388 hybrid zones like fitness changes along an ecological gradient or isolation by environment (Case
389 and Taper 2000; Case et al. 2005; McEntee et al. 2018). There is support for this hypothesis
390 given significant differences among niches for all adjacent pairs of lineages (Fig S3).
391

392 *Influence of barriers and environment on population structure*

These ratsnake lineages are structured by a complex of physical barriers, historical climate profiles, and geographic distance. Machine learning approaches show that the Mississippi River has served as a strong barrier for isolating lineages of ratsnakes, forming groups east and west of this river during the mid-Pleistocene at 1.08 My (95% CI =0.553 to 1.674 My; Figs 1&4, Table 1). These results are consistent with previous mtDNA and morphological conclusions (Burbrink, 2001; Burbrink et al., 2000). The Mississippi River has served as a strong barrier to gene flow given evidence from historical estimates of increased drainage (Cox et al. 2014) and numerous unrelated organisms show genetic disconnection across the river (Robison 1986; Burbrink 2002; Soltis et al. 2006; Burbrink et al. 2008; Pyron and Burbrink 2009; Brandley et al. 2010; Satler and Carstens 2017; Myers et al. 2020). Hybridization, while low (1-2 individuals/generation, Fig.3), does occur in a zone (~100km) east of the Mississippi River between the central lineages (*P. obsoletus* and *P. spiloides*; Fig. 6). Furthermore, divergence in this group can be predicted by elevation, geographic distance, and mid-Pleistocene climate change (787kya). The timing of the mid-Pleistocene climate change falls within the timing of divergence estimated from PipeMaster (Fig.4).

The Mississippi River is responsible for the earliest divergence in this complex but other geographic features are also important. East of the Mississippi River, divergence between *P. alleghaniensis* and *P. spiloides* was influenced by elevation, climate at the LGM, and geographic distance after accounting for variable inflation (Fig 4). For these taxa, divergence occurred at the Appalachian Mountains and Apalachicola/Chattahoochee River System, which suggests that changes in elevation at the Appalachian Mountains, in part, played a role in isolating lineages or maintaining divergence. Finer-scale testing is necessary to tease apart the effects of these river systems, ancient embayments, and connections to uplifted areas. Although the timing of

416 divergence predates the LGM, it is possible that repeated 100,000 year glacial cycles isolated
417 these taxa into refugia, as has been suggested previously for ratsnakes and other organisms
418 (Waltari et al. 2007; Noss et al. 2015). Alternatively, *Pantherophis alleghaniensis* may have
419 diverged in an isolated Florida, due to sea level changes during interglacials, and subsequently
420 expanded north and west. The concentration of the yellow, striped morphology in the range of *P.*
421 *alleghaniensis* in Florida and parts of the southeastern coast of the US indicates that this isolation
422 likely resulted in these morphologically unique taxa (Schultz 1996; Burbrink 2001). This area of
423 isolation, defined as a suture zone between the Florida peninsula and the continental US has been
424 found for many taxa (Remington 1968; Swenson and Howard 2005; Ruane et al. 2015). While
425 these two forms can be delimited with genetic data and occupy distinctly different geographic
426 regions, reproductive isolation is not complete. However, niches are significantly different and *P.*
427 *alleghaniensis* is typically found in the Florida peninsula and coastal plain environments (Bailey
428 1995; Burbrink 2001), whereas *P. spiloides* is found throughout the remainder of the forested
429 habitats east of the Mississippi River including the ecoregions defined as interior river valleys
430 and hills, interior plateau, Appalachian habitats, southeastern and southcentral plains, and
431 Mississippi River valley. Uncertainty in the identity of taxa using morphology where these taxa
432 meet is likely due to extensive gene flow in hybrid zones at barriers following postglacial range
433 expansion (Fig. 1, 3; Burbrink 2001; Gibbs et al. 2006).
434 Divergence between *P. bairdi* and *P. obsoletus* occurred in the western edge of the
435 Edwardas Plateau, with the former extending westward into xeric forested or Chihuahuan desert
436 scrub habitats always associated with rocky habitats, whereas the latter extends east into Texas,
437 preferring forested habitats, (Lawson and Lieb 1990; Werler and Dixon 2000). Population
438 genetic structure between these taxa is associated with mid-Pleistocene climate, elevation, and

439 geographic distance (Fig. 4). Dates of origin of these taxa are within the mid-Pleistocene,
440 suggesting that past climate played a strong role in promoting population divergence. During this
441 period, the Chihuahuan Desert was much drier relative to the late-Pleistocene (Graham and Mead
442 1987; Metcalfe et al. 2002; Metcalfe 2006) and this increased aridity could have driven
443 ecological divergence between this species pair. While divergence time is not the oldest here,
444 migration rates are lowest, and a hybrid zone is narrow. Previous research shows limited
445 hybridization with backcrosses between these taxa occurring in a narrow region of the
446 southwestern Edwards Plateau (Lawson and Lieb 1990; Vandewege et al. 2012).
447 Despite each lineage occupying uniquely different habitats, population responses to
448 Pleistocene climate change were similar (Fig. 3). Given the divergence time for each group, N_e
449 has expanded by 50 times since the Pleistocene. These estimates are consistent with other
450 predictions in the ENA, where 75% of the tested vertebrates show population size expansion and
451 75% of tested snakes show synchronous expansion of N_e, likely coinciding with the retreat of
452 glaciers at various times in the Pleistocene or during the Holocene (Bintanja and van de Wal
453 2008; Burbrink et al. 2016). However, *Pantherophis bairdi* has a range only in a small area of
454 the west Texas and isolated populations in northeastern Mexico, where habitats may have been
455 indirectly affected by glacial cycles.
456
457 *Taxonomy and delimitation in the genomic age*
458 Delimiting species using genetic data, while useful, has proved controversial (Bauer et al.
459 2011; Sukumaran and Knowles 2017; Leaché et al. 2019). In particular, most genetic
460 delimitation methods fail to account for gene flow (but see Flouris et al. 2019), do not consider
461 spatial information, and place individuals into predefined groups prior to testing (O'Meara

462 2010). These methods all assume species diverge at an evolutionary time scale where mutations
463 accumulate through drift or selection (Rannala 2015). And while simulations show that a
464 threshold above one migrating individual/10 generations will cause model-based delimitation
465 methods to fail at finding two species (Zhang et al. 2011), it is not clear how pulses or
466 inconsistent migration affect species transitioning through the gray zone. Importantly, Wright
467 (1931) indicated that up to 1,000 individuals migrating/generation may not prevent populations
468 from drifting given effective population size and spatial segregation.

469 Modern thresholds for species delimitation (Jackson et al. 2016; Leaché et al. 2019) use
470 GDI (>0.7), estimates of species divergence time over population size ($2\tau/\theta>1$), absolute
471 divergence time (10^4) and maximum migration rates ($M=Nm<1$), metrics that are all likely
472 influenced by sampling effort, location of samples sequenced, and detection of hybrids. For
473 example, if large hybrid zones exist but remain poorly sampled then estimates of migration will
474 be reduced, GDI will be high, and the probability of MSC estimators will suggest multiple
475 species. Conversely, if only hybrid zones are sampled then all metrics will predict only a single
476 species. For all pairs of ratsnakes $2\tau/\theta>1$ and divergence time is always greater than 10^4.
477 However, migration rates remain high between adjacent pairs in the eastern lineages. This forces
478 us to address how we are defining a species in the context of hybrid zones, how we infer
479 reproductive isolation beyond MSC methods, and how selection is maintaining hybrid zones. For
480 all lineages of ratsnakes, hybrid zones are smaller than predicted by neutral selection if these
481 hybrid zones formed in the Pleistocene. It is possible that these hybrid zones formed after the
482 retreat of the last glacial cycle during the Holocene. However, geographic lineage identity has
483 been maintained for >133,000 generations in all pairs, regardless of migration, and niches are
484 unique among all lineages. Moreover, where hybrid zones extend over large areas, gene flow

485 likely varies throughout space and may have changed over time (Barton and Hewitt 1985; Mallet
486 2007), particularly in response to glacial cycles. Thus, identifying and delimiting species in the
487 context of admixture is complex. Still, maintaining lineage and geographic identity, even with a
488 hybrid zone suggests that selection may have maintained unique evolutionary trajectories.

489 Here we have demonstrated that these four species, delimited previously using mtDNA
490 and morphology (Burbrink, 2001; Burbrink et al., 2000) can be recognized as distinct taxa given
491 methods of spatial grouping and species delimitation, though ranges in the eastern-most lineage
492 are restricted much further south than previously thought. However, migration rates between *P.*
493 *spiloides* and *P. alleghaniensis* (Fig. 3) are high enough to draw some concern that these taxa
494 should not be recognized given that they may not represent independent evolutionary trajectories
495 (de Queiroz, 2007; Rannala, 2015; Zhang et al., 2011). Unique niches in the subtropical areas of
496 the southeastern US and morphology provides some evidence for isolation between these taxa:
497 the striped forms (with variable ground colors of orange, yellow, green, and gray) are indicative
498 of *P. alleghaniensis* whereas adults with dark saddle patterns on grey, olive, brown, or black
499 ground colors (or completely black with no pattern) are found west of Florida and east of the
500 Mississippi River, throughout the Midwest and up to the northeastern US and Canada represent
501 *P. spiloides*. However, hybridization north and west of Florida is likely represented by a dulling
502 of this yellow ground color and mixed patterned individuals (Schultz 1996; see Supporting
503 Information Material 1 for more information on taxonomy).

504

505 *Future Directions*

506 To better understand the complexity of speciation processes, an even more integrated
507 whole-genomic approach with dense population sampling should be implemented. Even when

508 researchers have demonstrated that integrating spatial information along with estimates of timing
509 and gene-flow among groups presents a more comprehensive picture of speciation over a
510 complex landscape, there still remain several areas of investigation. For instance, estimating
511 gene flow and cline shape using detailed transects across various intersections along hybrid
512 zones would provide a better understanding of how migration changes in different habitats at
513 different latitudes and what type of hybrid zone is present. Additionally, better integrating
514 spatial, habitat, and migration estimates would allow researchers to test dynamic speciation
515 models that could be used to understand how migration changes over the landscape at various
516 times throughout the history of these taxa. Finally, using whole genome data along clines will
517 help determine if selection is occurring in the hybrid zones and determine the function of loci
518 showing evidence of selection and resisting gene flow.
519
520 **Author contributions:** FTB and EAM contributed to data collection, all authors contributed to
521 analyses, FTB wrote the initial draft, and all authors edited subsequent versions.
522
523 **Acknowledgments:** We thank R. Glor, R. Brown, and L. Welton at KU and C. Austin and D.
524 Dittman at LSUMN and K. Krysko and FLMNH, D. Shepard at Louisiana Tech University, and
525 A. McKelvy for providing tissues. We also thank L. and G. Derryberry for help with HZAR. We
526 also thank E. Chen for help extracting DNA. EAM was funded by the Gerstner Scholar/Theodore
527 Roosevelt and Peter Buck/Walter Rathbone Bacon fellowships. We thank D. Frost, A. Leaché,
528 A. Bauer, and K. deQuieroz for helpful discussions on species delimitation, type specimens, and
529 admixed type specimens.
530

Data Accessibility Statement: All data and unique scripts are available on Dryad XXX.

Literature Cited

Agrawal, A. F., J. L. Feder, and P. Nosil. 2011. Ecological Divergence and the Origins of Intrinsic Postmating Isolation with Gene Flow. Int. J. Ecol. 2011:1–15.

Bailey, R. G. 1995. Description of the ecoregions of the United States. 2nd ed. USDA Forest Service.

Bailey, R. I., M. R. Tesaker, C. N. Trier, and G.-P. Saetre. 2015. Strong selection on male plumage in a hybrid zone between a hybrid bird species and one of its parents. J. Evol. Biol. 28:1257–1269.

Barton, H. H., and K. Gale. 1993. Genetic analysis of hybrid zones. Pp. 13–45 *in* Hybrid Zones and the Evolutionary Process. Oxford University Press, New York.

Barton, N. H. 2010. What role does natural selection play in speciation? Philos. Trans. R. Soc. Lond. B. Biol. Sci. 365:1825–40.

Barton, N. H., and G. M. Hewitt. 1985. Analysis of Hybrid Zones. Annu. Rev. Ecol. Syst. 16:113–148.

Bauer, A. M., J. F. Parham, R. M. Brown, B. L. Stuart, L. Grismer, T. J. Papenfuss, W. Böhme, J. M. Savage, S. Carranza, J. L. Grismer, P. Wagner, A. Schmitz, N. B. Ananjeva, and R. F. Inger. 2011. Availability of new Bayesian-delimited gecko names and the importance of character-based species descriptions. Proc. R. Soc. B Biol. Sci. 278:490.

Beugin, M.-P., T. Gayet, D. Pontier, S. Devillard, T. Jombart, and T. Hansen. 2018. A fast

554 likelihood solution to the genetic clustering problem. Methods Ecol. Evol. 9:1006–1016.
555 Bintanja, R., and R. S. W. van de Wal. 2008. North American ice-sheet dynamics and the onset
556 of 100,000-year glacial cycles. Nature 454:869–72.
557 Bouckaert, R., J. Heled, D. Kühnert, T. Vaughan, C.-H. Wu, D. Xie, M. A. Suchard, A.
558 Rambaut, and A. J. Drummond. 2014. BEAST 2: A software platform for Bayesian
559 evolutionary analysis. PLoS Comput. Biol. 10:e1003537.
560 Bradburd, G. S., G. M. Coop, and P. L. Ralph. 2018. Inferring continuous and discrete
561 population genetic structure across space. Genetics 210:33–52.
562 Brandley, M. C., T. J. Guiher, R. A. Pyron, C. T. T. Winne, and F. T. Burbrink. 2010. Does
563 dispersal across an aquatic geographic barrier obscure phylogeographic structure in the
564 diamond-backed watersnake (*Nerodia rhombifer*)? Mol. Phylogenet. Evol. 57:552–560.
565 Branstetter, M. G., and J. T. Longino. 2019. Ultra-conserved element phylogenomics of New
566 World Ponera (Hymenoptera: Formicidae) illuminates the origin and phylogeographic
567 history of the endemic exotic ant Ponera exotica. Insect Syst. Divers. 3.
568 Brown, J. L., D. J. Hill, A. M. Dolan, A. C. Carnaval, and A. M. Haywood. 2018. PaleoClim,
569 high spatial resolution paleoclimate surfaces for global land areas. Sci. Data 5:180254.
570 Bryant, D., R. Bouckaert, J. Felsenstein, N. A. Rosenberg, and A. RoyChoudhury. 2012.
571 Inferring species trees directly from biallelic genetic markers: bypassing gene trees in a full
572 coalescent analysis. Mol. Biol. Evol. 29:1917–1932.
573 Burbrink, F. T. 2002. Phylogeographic analysis of the cornsnake (*Elaphe guttata*) complex as
574 inferred from maximum likelihood and Bayesian analyses. Mol. Phylogenet. Evol. 25:465–
575 476.
576 Burbrink, F. T. 2001. Systematics of the eastern ratsnake complex (*Elaphe obsoleta*). Herpetol.

Monogr. 1–53.

Burbrink, F. T., Y. L. Chan, E. A. Myers, S. Ruane, B. T. Smith, and M. J. Hickerson. 2016. Asynchronous demographic responses to Pleistocene climate change in Eastern Nearctic vertebrates. Ecol. Lett. 19:1457–1467.

Burbrink, F. T., F. Fontanella, R. A. Pyron, T. J. Guiher, C. Jimenez, and R. Alexander Pyron. 2008. Phylogeography across a continent: The evolutionary and demographic history of the North American racer (Serpentes : Colubridae : *Coluber constrictor*). Mol. Phylogenet. Evol. 47:274–288.

Burbrink, F. T., F. G. Grazziotin, R. A. Pyron, D. Cundall, S. Donnellan, F. Irish, J. S. Keogh, F. Kraus, R. W. Murphy, B. Noonan, C. J. Raxworthy, S. Ruane, A. R. Lemmon, E. M. Lemmon, and H. Zaher. 2020. Interrogating genomic-scale data for Squamata (lizards, snakes, and amphisbaenians) shows no support for key traditional morphological relationships. Syst. Biol. 69:502–520.

Burbrink, F. T., R. Lawson, and J. B. Slowinski. 2000. Mitochondrial DNA phylogeography of the polytypic North American rat snake (*Elaphe obsoleta*): A critique of the subspecies concept. Evolution (N. Y). 54:2107–2118.

Case, T. J., R. D. Holt, M. A. McPeek, and T. H. Keitt. 2005. The community context of species' borders: ecological and evolutionary perspectives. Oikos 108:28–46.

Case, T. J., and M. L. Taper. 2000. Interspecific competition, environmental gradients, gene flow, and the coevolution of species' borders. Am. Nat. 155:583–605.

Cox, R. T., D. N. Lumsden, and R. B. Van Arsdale. 2014. Possible relict meanders of the Pliocene Mississippi River and their implications. J. Geol. 122:609–622.

De Queiroz, K. 2007. Species concepts and species delimitation. Syst. Biol. 56:879–886.

600 Derryberry, E. P., G. E. Derryberry, J. M. Maley, and R. T. Brumfield. 2014. hzar : hybrid zone
601 analysis using an R software package. Mol. Ecol. Resour. 14:652–663.
602 Edwards, S., R. Hopkins, and J. Mallet. 2020. Speciation. Pp. 296–318 *in* S. Scheiner and D.
603 Mindell, eds. The Theory of Evolution. University of Chicago Press, Chicago.
604 Faircloth, B. C., J. E. McCormack, N. G. Crawford, M. G. Harvey, R. T. Brumfield, and T. C.
605 Glenn. 2012. Ultraconserved Elements Anchor Thousands of Genetic Markers Spanning
606 Multiple Evolutionary Timescales. Syst. Biol. 61:717–726.
607 Feder, J. L., S. P. Egan, and P. Nosil. 2012. The genomics of speciation-with-gene-flow. Trends
608 Genet. 28:342–350.
609 Flouris, T., X. Jiao, B. Rannala, and Z. Yang. 2019. A Bayesian implementation of the
610 multispecies coalescent model with introgression for phylogenomic analysis. Mol. Biol.
611 Evol., doi: 10.1093/molbev/msz296.
612 Frankham, R., J. D. (Jonathan D. . Ballou, and D. A. (David A. Briscoe. 2010. Introduction to
613 conservation genetics. Cambridge University Press.
614 Frantz, A. C., L. C. Pope, T. R. Etherington, G. J. Wilson, and T. Burke. 2010. Using isolation-
615 by-distance-based approaches to assess the barrier effect of linear landscape elements on
616 badger (Meles meles) dispersal. Mol. Ecol. 19:1663–1674.
617 Garrick, R. C., J. D. Banusiewicz, S. Burgess, C. Hyseni, and R. E. Symula. 2019. Extending
618 phylogeography to account for lineage fusion. J. Biogeogr. 46:268–278.
619 Gavrilets, S. 2004. Fitness landscapes and the origin of species. Princeton University Press.
620 Gay, L., P.-A. Crochet, D. A. Bell, and T. Lenormand. 2008. Comparing clines on molecular and
621 phenotypic traits in hybrid zones: a window on tension zone models. Evolution (N. Y).
622 62:2789–2806.

Gehara, M., A. A. Garda, F. P. Werneck, E. F. Oliveira, E. M. da Fonseca, F. Camurugi, F. d. M. Magalhães, F. M. F. M. Lanna, J. W. Sites, R. Marques, R. Silveira-Filho, V. A. São Pedro, G. R. Colli, G. C. Costa, and F. T. Burbrink. 2017. Estimating synchronous demographic changes across populations using hABC and its application for a herpetological community from northeastern Brazil. Mol. Ecol. 26:4756–4771.

Gibbs, H. L., S. J. Corey, G. Blouin-Demers, K. A. Prior, and P. J. Weatherhead. 2006. Hybridization between mtDNA-defined phylogeographic lineages of black ratsnakes (*Pantherophis sp.*). Mol. Ecol. 15:3755–3767.

Gourbière, S., and J. Mallet. 2010. Are species real? The shape of the species boundry with exponential failure, reinforcement, and the "missing snowball." Evolution (N. Y). 64:1–24.

Graham, R. W., and J. I. Mead. 1987. Environmental fluctuations and evolution of mammalian faunas during the last deglaciation in North America. Pp. 371–402 *in* North America and Adjacent Oceans During the Last Deglaciation. Geological Society of America, Boulder, Colorado 80301.

Harrison, R. G. 1993. Hybrid zones and the evolutionary process. Oxford University Press.

Hewitt, G. 2000. The genetic legacy of the Quaternary ice ages. Nature 405:907–913.

Hewitt, G. M. 2008. Speciation, hybrid zones and phylogeography - or seeing genes in space and time. Mol. Ecol. 10:537–549.

Hey, J. 2010. Isolation with migration models for more than two populations. Mol. Biol. Evol. 27:905–920.

Hey, J., and R. Nielsen. 2004. Multilocus methods for estimating population sizes, migration rates and divergence time, with applications to the divergence of *Drosophila pseudoobscura* and *D-persimilis*. Genetics 167:747–760.

646 Hijmans, R. J., J. van Etten, and J. Checg. 2014. Geographic Data Analysis and Modeling [R
647 package raster version 2.5-8]. Comprehensive R Archive Network (CRAN).
648 Jackson, N. D., B. C. Carstens, A. E. Morales, and B. C. O'Meara. 2016. Species delimitation
649 with gene flow. Syst. Biol. 66:799–812.
650 Jiggins, C. D., and J. Mallet. 2000. Bimodal hybrid zones and speciation. Trends Ecol. Evol.
651 15:250–255.
652 Jombart, T. 2008. adegenet: a R package for the multivariate analysis of genetic markers.
653 Bioinformatics 24:1403–1405.
654 Jombart, T., S. Devillard, and F. Balloux. 2010. Discriminant analysis of principal components: a
655 new method for the analysis of genetically structured populations. BMC Genet. 11:94.
656 Joseph, L., and T. Wilke. 2007. Lack of phylogeographic structure in three widespread
657 Australian birds reinforces emerging challenges in Australian historical biogeography. J.
658 Biogeogr. 34:612–624.
659 Karrenberg, S., X. Liu, E. Hallander, A. Favre, J. Herforth-Rahmé, and A. Widmer. 2019.
660 Ecological divergence plays an important role in strong but complex reproductive isolation
661 in campions (Silene). Evolution (N. Y). 73:245–261.
662 Kuhn, M. 2008. Caret: Classification and Regression Training Package. R package version 6.0-
663 77.
664 Lawson, R., and C. S. Lieb. 1990. Variation and hybridization in *Elaphe bairdi* (Serpentes:
665 Colubridae). J. Herpetol. 24:280.
666 Leaché, A. D., T. Zhu, B. Rannala, and Z. Yang. 2019. The spectre of too many species. Syst.
667 Biol. 68:168–181.
668 Legendre, P., and M. J. Fortin. 2010. Comparison of the Mantel test and alternative approaches

669 for detecting complex multivariate relationships in the spatial analysis of genetic data. Mol.
670 Ecol. Resour. 10:831–844.
671 Legendre, P., J. Oksanen, and C. J. F. ter Braak. 2011. Testing the significance of canonical axes
672 in redundancy analysis. Methods Ecol. Evol. 2:269–277.
673 Lek, S., M. Delacoste, P. Baran, I. Dimopoulos, J. Lauga, and S. Aulagnier. 1996. Application of
674 neural networks to modelling nonlinear relationships in ecology. Ecol. Modell. 90:39–52.
675 Lek, S., and J. F. Gue. 1999. Artificial neural networks as a tool in ecological modelling , an
676 introduction. 120:65–73.
677 Libbrecht, M. W., and W. S. Noble. 2015. Machine learning applications in genetics and
678 genomics. Nat. Rev. Genet. 16:321–332.
679 Lourenço, C. R., K. R. Nicastro, C. D. McQuaid, R. M. Chefaoui, J. Assis, M. Z. Taleb, and G. I.
680 Zardi. 2017. Evidence for rangewide panmixia despite multiple barriers to dispersal in a
681 marine mussel. Sci. Rep. 7:10279. Nature Publishing Group.
682 Makowsky, R., J. Chesser, and L. J. Rissler. 2009. A striking lack of genetic diversity across the
683 wide-ranging amphibian *Gastrophryne carolinensis* (Anura: Microhylidae). Genetica
684 135:169–183. Springer Netherlands.
685 Mallet, J. 2007. Hybrid speciation. Nature 446:279–283. Nature Publishing Group.
686 Mayr, E. 1963. Animal species and evolution. Belknap Press of Harvard University Press,
687 Cambridge,.
688 McEntee, J. P., J. G. Burleigh, and S. Singhal. 2018. Dispersal predicts hybrid zone widths
689 across animal diversity: Implications for species borders under incomplete reproductive
690 isolation. bioRxiv 472506. Cold Spring Harbor Laboratory.
691 Metcalfe, S. E. 2006. Late Quaternary environments of the northern deserts and central

transvolcanic belt of Mexico. Ann. Missouri Bot. Gard. 93:258–273. Missouri Botanical Garden Press.

Metcalfe, S., A. Say, S. Black, R. McCulloch, and S. O'Hara. 2002. Wet Conditions during the Last Glaciation in the Chihuahuan Desert, Alta Babicora Basin, Mexico. Quat. Res. 57:91–101.

Myers, E. A., A. D. McKelvy, and F. T. Burbrink. 2020. Biogeographic barriers, Pleistocene refugia, and climatic gradients in the southeastern Nearctic drive diversification in cornsnakes (*Pantherophis guttatus* complex). Mol. Ecol. 29:797–811. John Wiley & Sons, Ltd.

Myers, E. A., A. T. Xue, M. Gehara, C. L. Cox, A. R. Davis Rabosky, J. Lemos-Espinal, J. E. Martínez-Gómez, and F. T. Burbrink. 2019. Environmental heterogeneity and not vicariant biogeographic barriers generate community-wide population structure in desert-adapted snakes. Mol. Ecol. 28:4535–4548.

Nei, M. 1973. Analysis of gene diversity in subdivided populations. Proc Natl Acad Sci USA 70:3321–3323.

Nosil, P. 2012. Ecological Speciation. Oxford University Press, Oxford.

Nosil, P., and B. J. Crespi. 2006. Ecological divergence promotes the evolution of cryptic reproductive isolation. Proc. R. Soc. B-Biological Sci. 273:991–997.

Nosil, P., J. L. Feder, S. M. Flaxman, and Z. Gompert. 2017. Tipping points in the dynamics of speciation. Nat. Ecol. Evol. 1:1. Nat Ecol Evol.

Noss, R. F., W. J. Platt, B. A. Sorrie, A. S. Weakley, D. B. Means, J. Costanza, and R. K. Peet. 2015. How global biodiversity hotspots may go unrecognized: lessons from the North American Coastal Plain. Divers. Distrib. 21:236–244.

O'Meara, B. C. 2010. New heuristic methods for joint species delimitation and species tree inference. Syst. Biol. 59:59–73.

Orr, H. A. 1995. The population genetics of speciation: the evolution of hybrid incompatibilities. Genetics 139:1805–13. Genetics Society of America.

Paradis, E., and K. Schliep. 2019. ape 5.0: an environment for modern phylogenetics and evolutionary analyses in R. Bioinformatics 35:526–528. .

Petkova, D., J. Novembre, and M. Stephens. 2016. Visualizing spatial population structure with estimated effective migration surfaces. Nat. Genet. 48:94–100. Nature Publishing Group.

Plummer, M., N. Best, K. Cowles, and K. Vines. 2006. CODA: Convergence diagnosis and output analysis for MCMC. R News 6:7–11.

Pyron, R. A., and F. T. Burbrink. 2009. Lineage diversification in a widespread species: roles for niche divergence and conservatism in the common kingsnake, Lampropeltis getula. Mol. Ecol. 18:3443–3457.

Rannala, B. 2015. The art and science of species delimitation. Curr. Zool. 61:846–853.

Remington, C. L. 1968. Suture-zones of hybrid interaction between recently joined biotas. Pp. 321–428 *in* Evolutionary Biology. Springer US, Boston, MA.

Riddle, B. R. 2016. Comparative phylogeography clarifies the complexity and problems of continental distribution that drove A. R. Wallace to favor islands. Proc. Natl. Acad. Sci. U. S. A. 113:7970.

Robison, H. W. 1986. Zoogeographic implications of the Mississippi River Basin. Pp. 267–285 *in* The Zoogeography of North American Freshwater Fishes. Wiley, New York.

Roux, C., C. Fraïsse, J. Romiguier, Y. Anciaux, N. Galtier, and N. Bierne. 2016. Shedding light on the grey zone of speciation along a continuum of genomic divergence. PLoS Biol.

738 14:e2000234.
739 Ruane, S., O. Torres-Carvajal, and F. T. Burbrink. 2015. Independent demographic responses to
740 climate change among temperate and tropical milksnakes (Colubridae: Genus
741 *Lampropeltis*). PLoS One 10:e0128543.
742 Satler, J. D., and B. C. Carstens. 2017. Do ecological communities disperse across biogeographic
743 barriers as a unit? Mol. Ecol. 26:3533–3545.
744 Schultz, K. D. 1996. A monograph of the colubrid snakes of the genus *Elaphe* Fitzinger. Koelz
745 Scientific Books, Havlicuv.
746 Seehausen, O., R. K. Butlin, I. Keller, C. E. Wagner, J. W. Boughman, P. A. Hohenlohe, C. L.
747 Peichel, G.-P. Saetre, C. Bank, A. Brannstrom, A. Brelsford, C. S. Clarkson, F.
748 Eroukhmanoff, J. L. Feder, M. C. Fischer, A. D. Foote, P. Franchini, C. D. Jiggins, F. C.
749 Jones, A. K. Lindholm, K. Lucek, M. E. Maan, D. A. Marques, S. H. Martin, B. Matthews,
750 J. I. Meier, M. Most, M. W. Nachman, E. Nonaka, D. J. Rennison, J. Schwarzer, E. T.
751 Watson, A. M. Westram, and A. Widmer. 2014. Genomics and the origin of species. Nat
752 Rev Genet 15:176–192.
753 Sheehan, S., Y. S. Song, E. Buzbas, D. Petrov, A. Boyko, and A. Auton. 2016. Deep learning for
754 population genetic inference. PLOS Comput. Biol. 12:e1004845.
755 Singhal, S., and C. Moritz. 2013. Reproductive isolation between phylogeographic lineages
756 scales with divergence. Proceedings. Biol. Sci. 280:20132246.
757 Soltis, D. E., A. B. Morris, J. S. McLachlan, P. S. Manos, and P. S. Soltis. 2006. Comparative
758 phylogeography of unglaciated eastern North America. Mol. Ecol. 15:4261–4293.
759 Stankowski, S., J. M. Sobel, and M. A. Streisfeld. 2017. Geographic cline analysis as a tool for
760 studying genome-wide variation: a case study of pollinator-mediated divergence in a

761 monkeyflower. Mol. Ecol. 26:107–122.
762 Sukumaran, J., and L. L. Knowles. 2017. Multispecies coalescent delimits structure, not species.
763 Proc. Natl. Acad. Sci. U. S. A. 114:1607–1612.
764 Sun, K., K. A. Meiklejohn, B. C. Faircloth, T. C. Glenn, E. L. Braun, and R. T. Kimball. 2014.
765 The evolution of peafowl and other taxa with ocelli (eyespots): a phylogenomic approach.
766 Proc. R. Soc. B Biol. Sci. 281:20140823.
767 Swenson, N. G., and D. J. Howard. 2005. Clustering of contact zones, hybrid zones, and
768 phylogeographic breaks in North America. Am. Nat. 166:581–591.
769 Vandewege, M. W., D. Rodriguez, J. P. Weaver, T. D. Hibbitts, M. R. J. Forstner, and L. D.
770 Densmore. 2012. Evidence of hybridization between *Elaphe bairdi* and *Elaphe obsoleta*
771 *lindheimeri* including comparative population genetics inferred from microsatellites and
772 mitochondrial DNA. J. Herpetol. 46:56–63. Society for the Study of Amphibians and
773 Reptiles.
774 Vavrek, M. J. 2020. Fossil. https://cran.r-project.org/web/packages/fossil/index.html.
775 Walker, D., and J. C. Avise. 1998. Principles of phylogeography as illustrated by freshwater and
776 terrestrial turtles in the southeastern United States. Annu. Rev. Ecol. Syst. 29:23–58.
777 Waltari, E., R. J. Hijmans, A. T. Peterson, Á. S. Nyári, S. L. Perkins, and R. P. Guralnick. 2007.
778 Locating Pleistocene refugia: comparing phylogeographic and ecological niche model
779 predictions. PLoS One 2:e563.
780 Werler, J. E., and J. R. Dixon. 2000. Texas snakes : identification, distribution, and natural
781 history. 1st ed. University of Texas Press, Austin.
782 Wright, S. 1978. Evolution and the Genetics of Populations. Vol. 4. Variability within and
783 among Natural Populations. University Chicago Press.

Wright, S. 1931. Evolution in Mendelian populations. Genetics 16:97–159.

Wright, S. 1943. Isolation by Distance. Genetics 28:114–38. Genetics Society of America.

Younger, J. L., P. Dempster, Á. S. Nyári, T. O. Helms, M. J. Raherilalao, S. M. Goodman, and S. Reddy. 2019. Phylogeography of the Rufous vanga and the role of bioclimatic transition zones in promoting speciation within Madagascar. Mol. Phylogenet. Evol. 139:106535.

Zellmer, A. J., M. M. Hanes, S. M. Hird, and B. C. Carstens. 2012. Deep phylogeographic structure and environmental differentiation in the carnivorous plant Sarracenia alata. Syst. Biol. 61:763–777.

Zhang, C., D.-X. Zhang, T. Zhu, and Z. Yang. 2011. Evaluation of a bayesian coalescent method of species delimitation. Syst. Biol. 60:747–761.

Zhang, W. 2010. Computational Ecology: Artificial Neural Networks and Their Applications. World Scientific.

807 Table 1. Measures of divergence dates in millions of years (My), migration rates (first number is
808 first taxon into second taxa, e.g., *Pantherophis alleganiensis* into *P.spiloides*, and second vice
809 versa), and migration rates (individuals/generation) for each contacting group in the
810 *Pantherophis obsoletus* complex.
811

Group	**Age (My)**	**Migration Rate (ind/gen)**	**Cline Width (m)**
Eastern (*P. alleghaniensis* x *P.spiloides*)	0.65 (0.367-0.875)	2.79/3.79	125 (114-138)
Central (*P.spiloides* x *P.obsoletus*)	1.08 (0.55-1.67)	1.96/1.28	97 (88-107)
Western (*P.obsoletus* x *P. bairdi*)	0.367 (0.37-0.88)	0.65/0.55	8 (4-15)

812

Figures and Legends

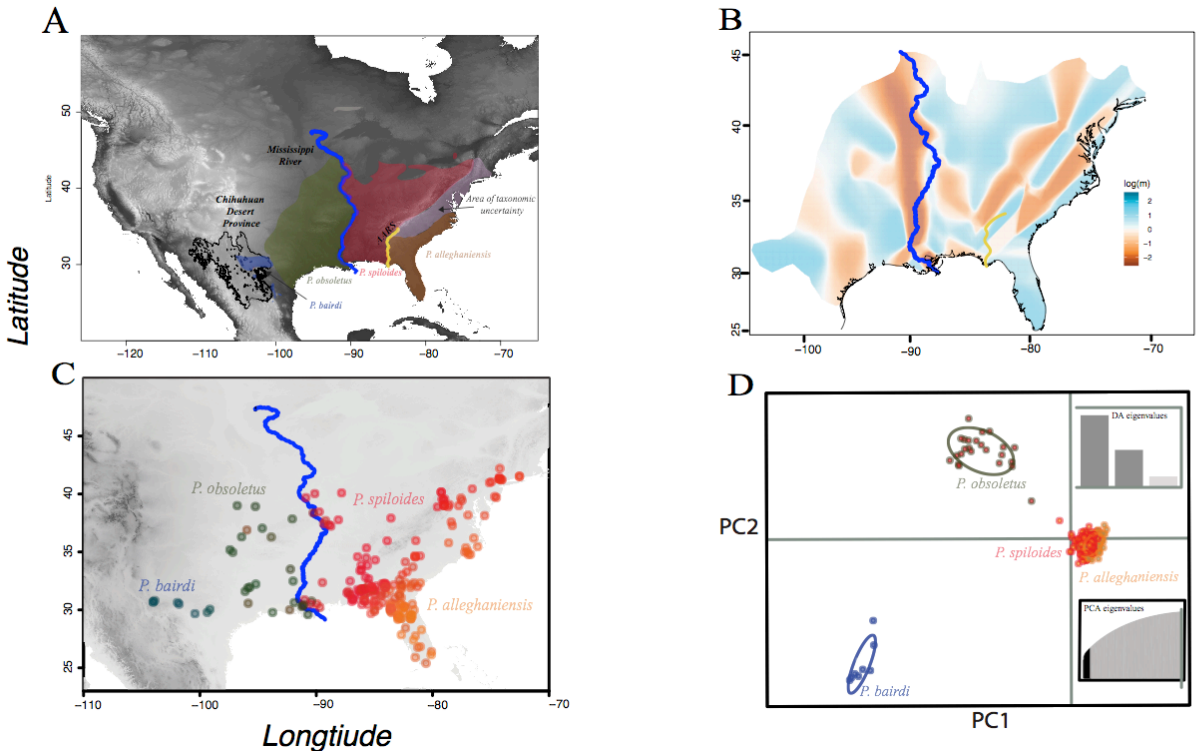

Fig.1. Distribution and population delimitation for the ratsnakes *Pantherophis obsoletus* complex. (A) Map showing range and geographic features: Chihuahuan Desert Province, the Mississippi River, and the Appalachian Mountains and Apalachicola/Chattahoochee River System (AARS). (B) Estimated effective migration surfaces (EEMS) showing areas of both high (blue) and low migration (brown). (C) Population structure using Discriminant Analysis of Principal Components (DAPC) shows the location of four geographically distinct lineages. (D) Bi-plots of PC space shows relative distances among the four taxa using DAPC.

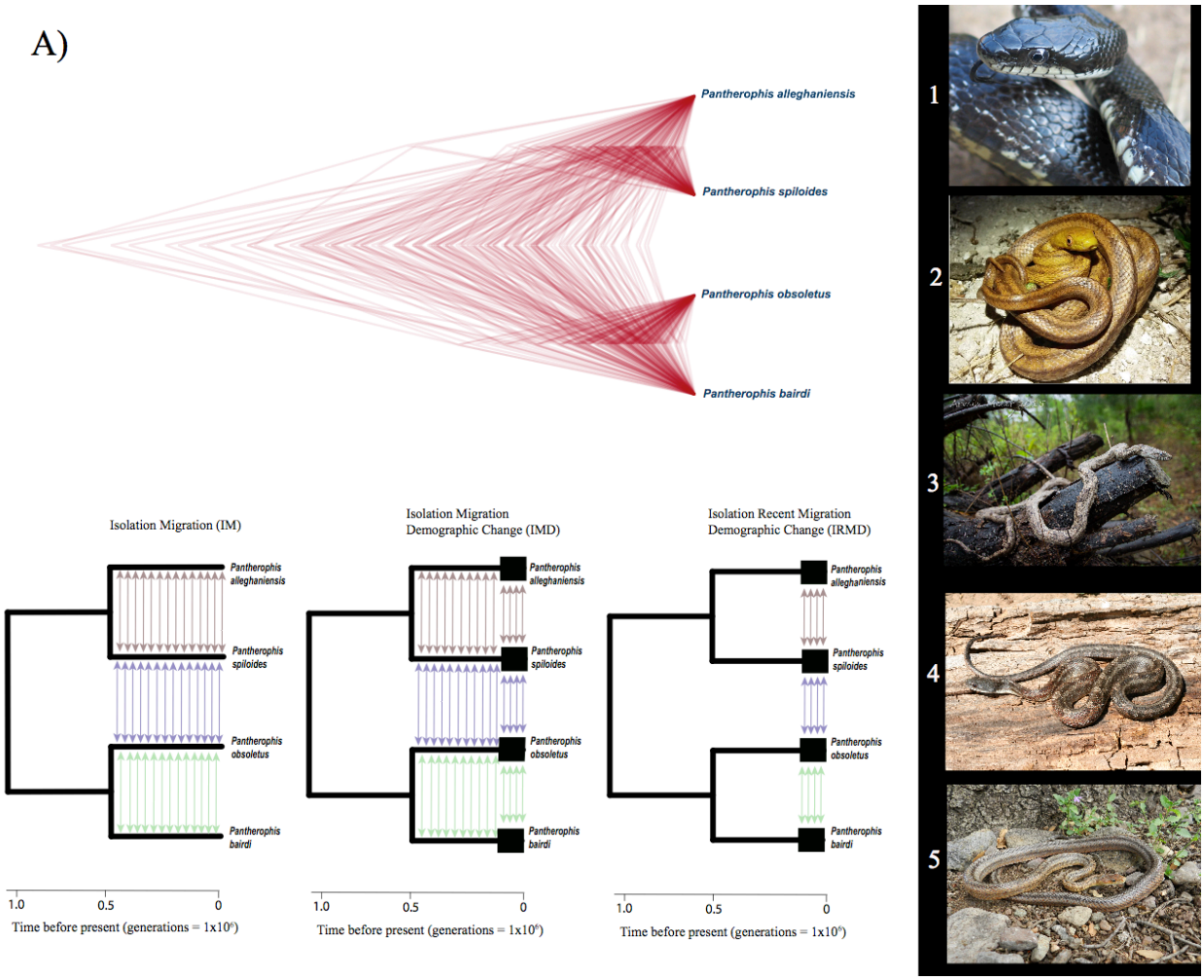

Fig.2. The results of SNAPP species-tree estimation for the four taxa over all loci (A) and models showing Isolation Migration (IM) and Isolation Migration with Demographic Change (IMD; best-fit model) and Isolation with Recent Migration and Demographic Change (IMRD) estimated in PipeMaster. Colored arrows represent migration among spatially adjacent pairs. (B). Photographs representing some of the typical color patterns seen in ratsnakes: 1) *Pantherophis alleghaniensis* (photo F. Burbrink), 2) *P. alleghaniensis* (photo N. Claunch), 3) *P. spiloides* (photo A. Meier), 4) *P. obsoletus* (photo D. Shepard), and 5) *P. bairdi* (E. Myers).

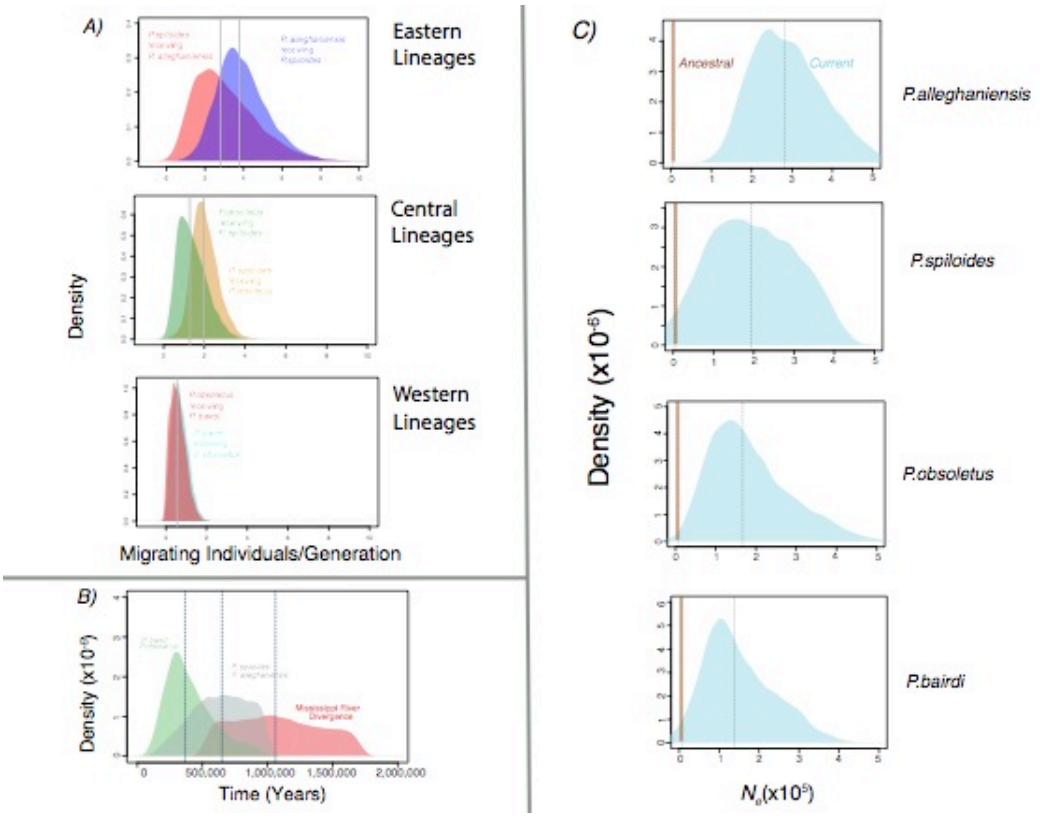

Fig.3. Results from PipeMaster showing estimates and directionality of gene flow (A), divergence times between groups and taxon pairs (B), and changes in population sizes over time (C).

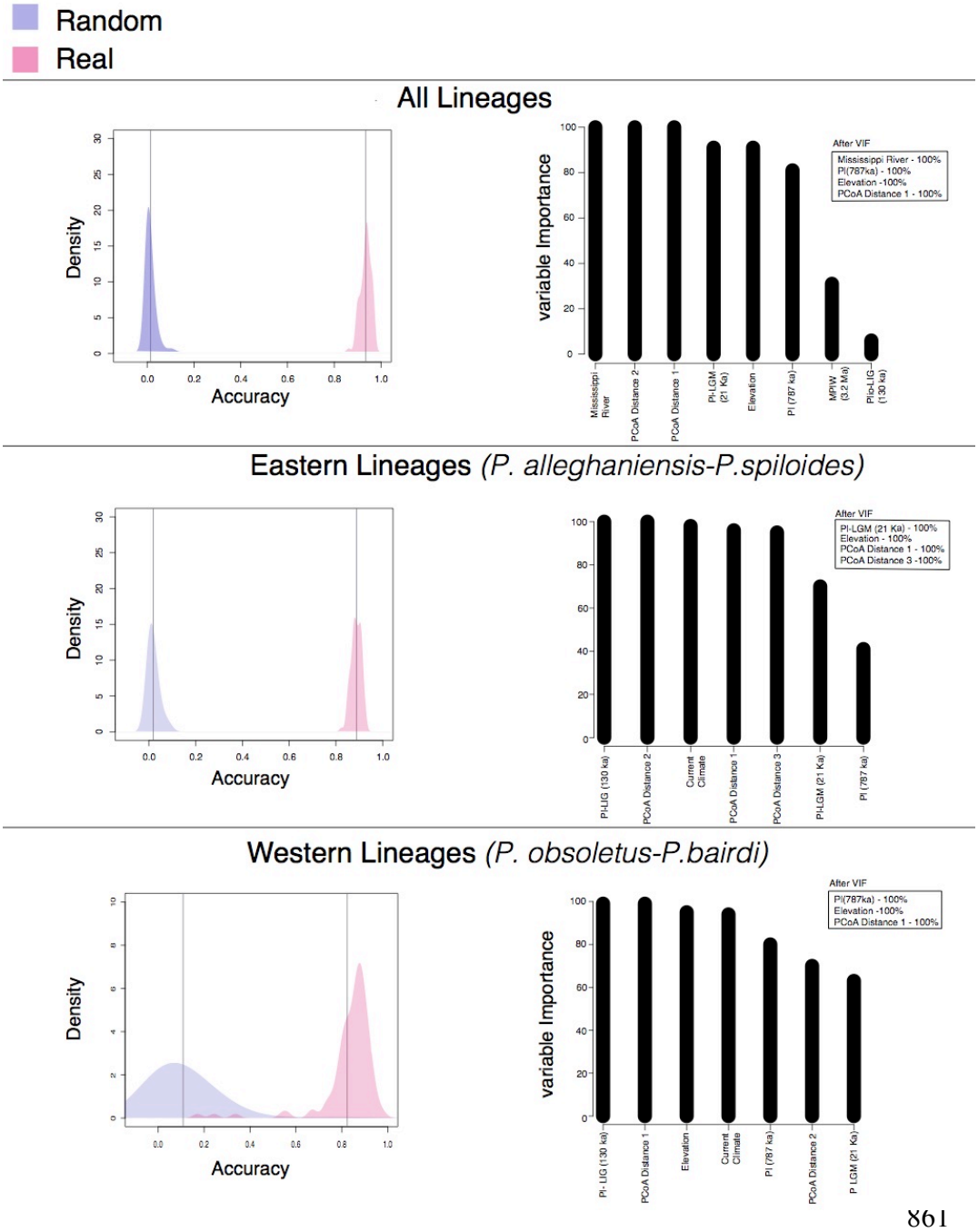

Fig.4. Artificial neural network results showing accuracy predicting genetic structure among all lineages and species pairs (left) and ranked variable importance (filtered for multicollinearity in inset box, right).

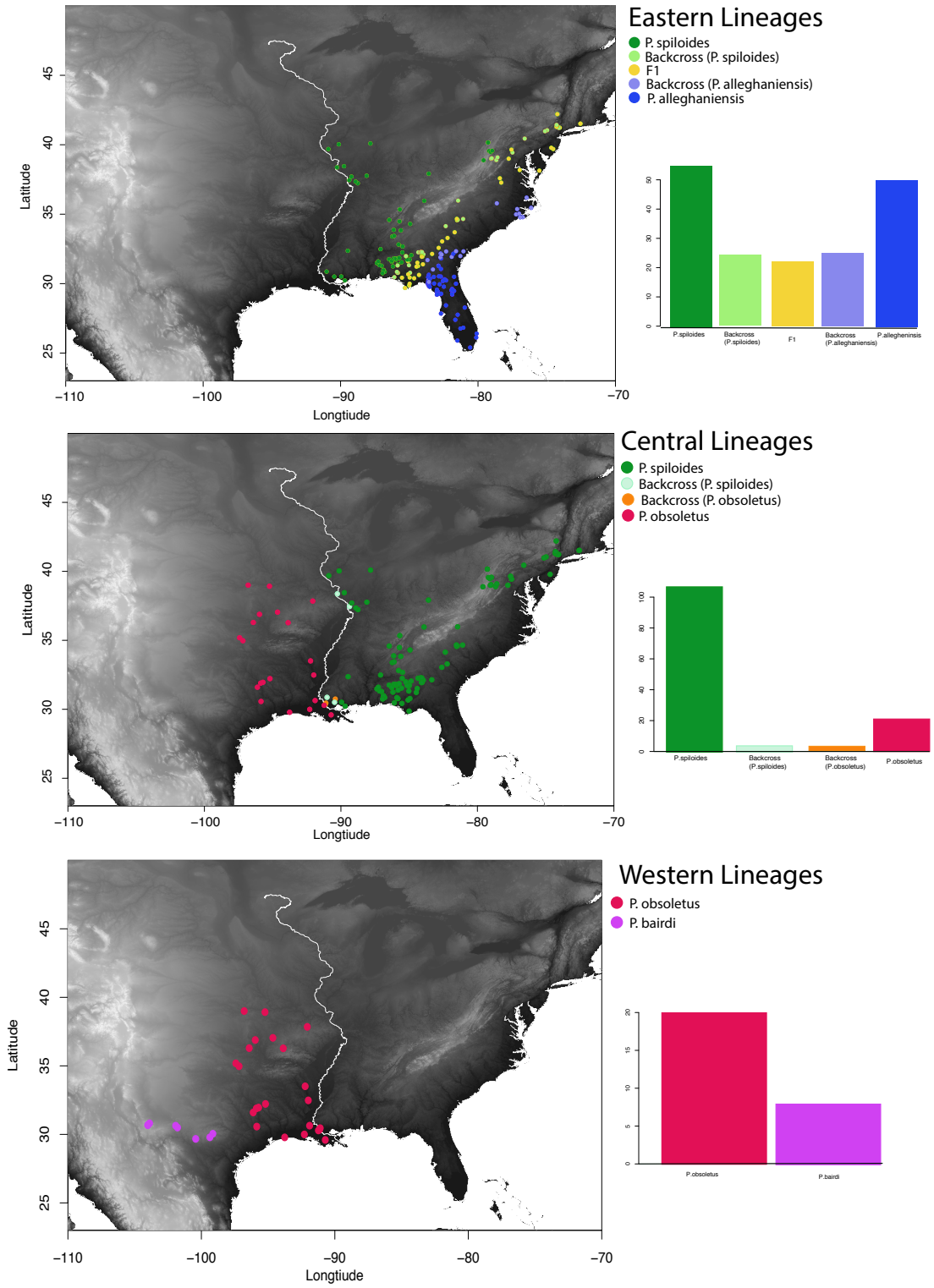

865

866 Fig.5. Results from estimating hybrid types between taxon pairs using *snapclust* showing the

867 spatial distribution of parentals and hybrids along with their frequencies.

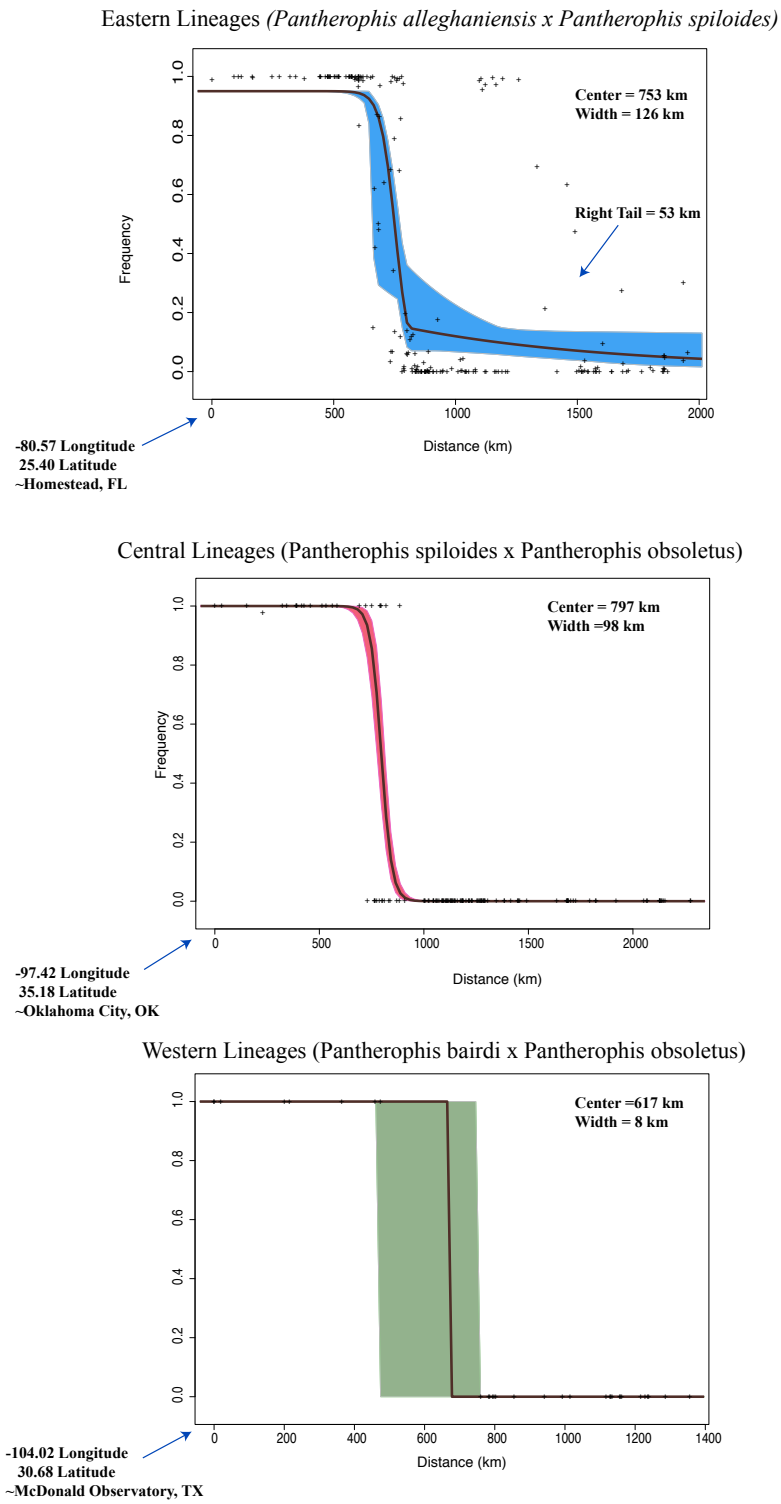

Fig.6. Cline model results for all three species pairs using Gaussian Cline (HZAR) model given locations and admixture estimates using DAPC.

871 **Supplemental Material**

872 DRYAD XXX

873 Genomic Dataset

874 Geographic Localities

875 R scripts

876

877 Supporting Information Material 1

878 Additional Methods

879

880 Table S1 – Priors and summary stats for PipeMaster; estimating migration, timing of divergence,

881 and historical demography

882 Table S2 – PHRAPL Results (*open with R read.table() or Excel*)

883 Table S3 – RDA and ANN Results

884 Table S4 – HZAR Results for *snapclust* assignments

885 Table S5 – HZAR results for DAPC assignments

886

887 Fig.S1. Delimiting populations using sparse nonnegative matrix factorization (SNMF) and

888 spatial Principal Component analysis (sPCA) showing the location of four geographically

889 distinct lineages.

890

891 Fig. S2 – PipeMaster model fit of observed data to simulations under IM, IMD, and IMD-LGM

892 models for PC1-PC10.

893

894 Fig. S3 – Symmetric background niche similarity tests for spatially adjacent pairs (eastern,
895 central, and western lineage comparisons) for the *D* and *I* statistics.
896
897 Fig. S4 – Prediction of cline width under neutrality given origin times for each species pair: A)
898 *Pantherophis alleghaniensis/P. spiloides*, B) *P. spiloides/P.obsoletus*, and C) *P.*
899 *obsoletus/P.bairdi.*
900
901
902 **Supporting Information Material 1**
903 **Supplemental Methods and Results**
904
905 *Dataset*
906
907 We sampled 288 individuals liberally covering the range of all species within the
908 *Pantherophis obsoletus* complex (Fig.1; Dryad XXX). DNA was extracted from all samples
909 using Qiagen DNeasy Blood & Tissue Kits and samples were screened for quality using broad-
910 range Qubit Assays (https://www.thermofisher.com/us/en/home/industrial/spectroscopy-
911 elemental-isotope-analysis/molecular-spectroscopy/fluorometers/qubit/qubit-assays.html). We
912 used services from RAPiD Genomics (https://www.rapid-genomics.com/services/) to generate
913 5472 baits and to sequence 5060 conserved elements (UCEs) loci following the protocols from
914 (Faircloth et al., 2012) and (Sun et al., 2014).
915 Raw sequence reads were trimmed of adapter contamination using illumiprocessor
916 (Faircloth, 2013), a wrapper around the trimmomatic package (Bolger et al., 2014). These

917 sequence capture data were then assembled by mapping reads to all UCEs found within a
918 Chromium 10x assembled *Pantherophis spiloides* genome (Burbrink and Myers, *in prep*) after
919 2,500 base pairs of flanking DNA around UCE baits were pulled from this genome assembly
920 using the Phyluce commands *phyluce_probe_run_multiple_lastzs_sqlite* and
921 *phyluce_probe_slice_sequence_from_genomes* (Faircloth, 2016). Sequence reads for each
922 sample were then mapped to the 'reference' UCE dataset using bwa v0.7.17 (Li and Durbin,
923 2009). Samtools was used to convert sam format to bam files and alignments were soft clipped
924 using the CleanSam tool in Picard (http://broadinstitute.github.io/picard/). To phase these data,
925 we mapped reads back to each individual sample's alignments. To do this, bam files were
926 converted to fastq using samtools mpileup (Li et al., 2009), fastq files were converted to fasta
927 format via seqtk (https://github.com/lh3/seqtk) and all missing sites were removed using seqkit
928 (Shen et al 2016). These newly created fasta files were then used as a reference sequence for
929 phasing the data following the seqcap_pop pipeline (Harvey et al., 2016). Briefly we followed
930 this pipeline and used GATK (McKenna et al., 2010) to mark duplicates, call, realign, and
931 annotate/mask indels, call and annotate SNPs via GATK, restrict SNP calling to high quality
932 SNPs, and then conducted read backed phasing. Finally, we created a sample specific fasta file of
933 all phased loci for every sample using 'add_phased_snps_to_seqs_filter.py' available via the
934 seqcap_pop pipeline (Harvey et al., 2016). All samples were combined into locus specific fasta
935 files using a perl script developed in (Myers et al., 2019). Locus specific fasta files were aligned
936 using muscle as implemented in the R package ape (Paradis and Schliep, 2019) after removing
937 individuals from alignments that fell below the 25% quantile of the distribution of sequence
938 lengths for each locus. All fasta files were conservatively trimmed of missing data resulting in
939 alignments with no missing sites (i.e., trimming to the shortest sequence in the alignment). We

940 filtered these alignments by removing all loci that were missing >50% sequenced samples and
941 removed all individuals that were missing from >30% of all alignments. Finally, we created a vcf
942 file from these alignments and using vcftools (Danecek et al., 2011) and filtered this for minor
943 allele frequency >10% retaining only 1 SNP/locus for population assignment analyses (Linck
944 and Battey, 2019).
945
946
947 *Geographic groupings*
948 We estimated population structure by comparing Discriminant Analysis of Principal Components
949 (DAPC; Jombart et al., 2010) and spatial Principal Component analysis (sPCA; Jombart et al.,
950 2008) in adegenet v2.1.2(Jombart 2008), sparse nonnegative matrix factorization (SNMF;
951 Frichot et al., 2014) in LEA v1.4.0 (Frichot and François 2015), and estimated effective
952 migration surfaces (EEMS v; Petkova et al., 2016), which accounts for IBD . Each of these
953 methods use different assumptions for grouping individuals and we compare congruence among
954 them.The model-free method DAPC sequentially estimates K-means for clustering and selects
955 the best fit to infer genetic clusters in the absence of prior group identification. Using the
956 package adegenet (Jombart 2008) in R (R Core Team 2015) we first transformed data using PCA
957 by choosing a large number of PC axes (n=200), then picking the number of discriminant
958 functions yielding large F-statistics (>2000) and optimal number of groups using BIC (Bayesian
959 inference criterion). Because using a large number of the PCs may yield arbitrary solutions, we
960 estimated the optimal *a-score*, which measures this bias by calculating the difference between
961 the actual cluster assignment probabilities and randomly assigned probabilities (predicting 15-23

962 PCs). We also used cross-validation with a 90% training and 10% test dataset to estimate the
963 average predicted success for each group.

964 Because DAPC does not account for spatial structure, such as IBD, we also used sPCA.
965 Similar to DAPC, this method does not require data to be in Hardy-Weinberg or linkage
966 equilibrium. sPCA also adds an element of space by isolating global structure, representing
967 disconnected groups or clines, from local structure, representing repulsion (selection against
968 similar genetic types co-occurring), and random noise. Using adegenet, we estimated sPCA
969 given SNPs and locations of each sample using up to 15 positive eigenvalues (global structures)
970 and 15 negative eigenvalues (local structures). To connect individual locations to build a
971 connection network, we used Delaunay triangulation. We also implemented Monte-Carlo tests
972 with 100 permutations using the function *spca_randtests* to determine if significant local or
973 global spatial structures exist.

974 We also assessed ancestral coefficients using SNMF in the package LEA (Frichot and
975 François 2015). This methodology is comparable to ADMIXTURE (Alexander et al. 2009) and
976 Structure (Pritchard et al. 2000) methods, but runs 10-30x faster using genomic-scale data. This
977 method produces a least-squares estimate of ancestry populations given *K* ancestral populations
978 We estimated ancestry coefficients over 1-6 *K* using 100 repetitions per *K*, 100 iterations per
979 algorithm, and a tolerance of 0.05. To determine the appropriate number of groups, we used a
980 cross-validation technique with the entropy criterion, which masks genotypes to fit a particular
981 model to each *K*.

982 Finally, to compare these methods of grouping individuals into populations, we estimated
983 migration rates over the landscape using EEMS (Petkova et al. 2016). This method models
984 effective migration rates over geography to represent regions where migration is low in cases

985 when genetic dissimilarity increases rapidly, thus providing a uniquely distinct view of the
986 location of population clusters relative to biogeographic barriers as compared to DAPC, sPCA,
987 and SNMF. We ran EEMS 3 times for $3x10^6$ generations with burnin set at $1x10^6$ generations,
988 thinned by 9,999 generations, with 1,000 demes covering the known range of the *P. obsoletus*
989 complex (Burbrink 2001).

990 Both EEMS and DAPC find population structure, generally matched the geographic
991 ranges of *P. alleghaniensis*, *P. spiloides, P. obsoletus*, and *P. bairdi* (Fig. 1 and Fig. S1;
992 Burbrink, 2001). Total DAPC assignment probabilities were 0.975 (*P. bairdi* = 1.0, *P. obsoletus*
993 = 0.96; *P. spiloides* = 1.0, and *P. alleghaniensis* = 0.97). Comparing these assignments to those
994 from SMNF, we found that only *P. alleghaniensis* was misclassified as *P. spiloides* 8.5% of the
995 time. Similarly, SNMF cross validation predicted four groups (cv = 0.599) as compared to two
996 (cv=0.627), three (cv=0.607), and five (cv=0.601). These four groups generally match the same
997 ranges as those found in DAPC. sPCA showed the presence of four groups, with PC1 showing
998 the separation of groups at the MR and the two lineages east of this river, whereas PC2-5 shows
999 divergence in all taxa. Importantly, global spatial structures were significant (observed spatial
1000 structure test statistic = 75.47, random expectation = 28.14; $P < 0.009$). Similarly, all three
1001 EEMS runs suggest low migration at the MR and the area separating the *P. bairdi* and *P.*
1002 *obsoletus* in west Texas. East of the MR, estimated low migration occurred near the Appalachian
1003 Mountains, though this area is a complex mixture of isolation and gene flow (Fig. 1). All three
1004 EEMS generated similar acceptance proportions for all proposal types (12-51%).
1005
1006 *Running SNAPP*

1007 We set forward and reverse mutation rates to 1. We applied a gamma distribution ($\alpha = 2$, $\beta = 200$)
1008 for the speciation rate (λ) prior and the *snapprior* was set to $\alpha = 1$, $\beta = 250$, and $\kappa = 1$. To test the
1009 four alternative species delimitation models including four taxa, three taxa (collapsing *P.*
1010 *bairdi/P. obsoletus* or *P. alleghaniensis/P. spiloides*), and two taxa (collapsing *P. bairdi/P.*
1011 *obsoletus* and *P.alleghaniensis/P. spiloides* we used a stepping-stone analysis with the
1012 *PathSampleAnalyser* with 72 steps and a chain length of 200000, burnin percentage at 50%, and
1013 a preBurnin of 10,000. We checked for stationarity using Tracer v1.7.1 (Drummond and
1014 Rambaut 2007) determining that estimated sample size (ESS) were > 200 for all parameters.
1015 *Running PHRAPL*
1016 PHRAPL uses gene-tree distances between simulated and empirical data to rank models using
1017 approximate likelihoods and AICs. To generate the empirical observations we estimated
1018 unrooted gene trees for each loci using IQ-Tree 1.6.12 (Nguyen et al. 2015) and testing all
1019 substitution models per locus prior to estimation. We rooted the trees using midpoint rooting and
1020 performed 100 subsamples of two individuals per population. To reduce model space, we
1021 allowed only one population size parameter (all populations have equal size) and one migration
1022 parameter (all migration rates are equal). We then ran 1000 simulations per model, searching
1023 over a grid of four CollapseStarts values and five MigrationStarts values.
1024
1025 *Niche models*
1026 We determined if the four taxa show uniquely distinct niches. We quantified niche
1027 similarity using methods introduced in Warren et al. (2008) using Schoener's *D* and Hellinger
1028 distance *I* (Schoener 1968). We used the georeferenced genetic samples here as inputs,
1029 predictions of species identity from DAPC, and 19 bioclimatic variables cropped to the eastern

1030 half of the US (Fick and Hijmans 2017). Estimates of *D* and *I* between adjacent species pairs
1031 were calculated and significance of niche identity was derived from 500 random permutations of
1032 lineage identity and re-estimation of the ecological niche model (ENM) using maxent (Phillips
1033 and Dudik 2008) in the R program ENMTools (Warren et al. 2010). Because underlying
1034 differences between lineage-pair regions may not be different from the exact locations of
1035 individuals estimating niche identity we used the background test to produce a null distribution
1036 of ENM symmetrically between a lineage and randomized occurrence points within the adjacent
1037 range of the other adjacent lineage (using a radius of 20km and 1000 points). Therefore, if *D* and
1038 *I* from the identity tests were significantly lower than the background test null distribution then
1039 similarity between species, provided that accessible habitat exists in the region, is rejected
1040 (Warren et al. 2008).
1041 Identity tests for niche overlap for both the *D* and *I* statistics were significant ($P <$
1042 $1.6 \times 10^{-12} – 4.02 \times 10^{-214}$) for all adjacent pairs. Dissimilarity for the background tests was
1043 significantly lower than the null distributions for all pairs of taxa (P=0.003 to 0.019; Fig. S3).
1044 These results suggests niches overlap between pairs of taxa less than expected by chance.
1045
1046
1047 *Spatial genetics using RDA*
1048 We predicted genetic distances from environmental, elevation, river, and distance variables using
1049 RDA in the R package Vegan (Dixon 2003), which avoided problems with spatial data using
1050 Mantel tests (Legendre et al. 2015). This method was used to compare results from the ANN
1051 analyses. RDA is an asymmetric canonical analysis here used to determine the significance of
1052 predictor axes (Legendre et al. 2011) at generating predict genetic structure over a landscape

1053 (McGaughran et al. 2014; Noguerales et al. 2016). We ran this using the *capscale* function where
1054 dissimilarity data were ordinated with metric scaling and then passed to RDA. All variable
1055 distances were used to predict genetic distance and significance of each variable was tested using
1056 anova-like permutation tests to examine the joint effect of predictor variables given partial
1057 effects from spatial distance to account for IBD. Also, given that some of these variables might
1058 be correlated, we assessed multicollinearity and reran RDA using the reduced number of
1059 predictor variables. To examine how multicollinearity among variables affects model inference
1060 given linear dependence among these independent variables (De Veaux and Ungar 1994; Hastie
1061 et al. 2001; Shan et al. 2006; Dormann et al. 2013), we used stepwise variable inflation factors in
1062 the package Rnalytica (https://rdrr.io/github/software-analytics/Rnalytica/). The function
1063 *stepwise.vif* selects non-correlated variables by excluding those with the highest variable
1064 inflation factor above five.

1065 Estimates of accuracy using ANN were high (>90%) for all comparisons and yielded
1066 similar conclusions to RDA. Here, RDA demonstrated that most of the structure for all taxa can
1067 be predicted by the Mississippi River, MIS19 (climate at 787Kya), and elevation (P=0.001-
1068 0.002) and these predictors similarly showed 100% variable importance using ANN (Table S3).
1069 Distance also played a role in structuring these data, though they were partialed out in RDA. For
1070 those lineages east of the MR, population structure was predicted by LGM and elevation (RDA:
1071 P = 0.001, ANN: variable importance=100). For those lineages west of the MR, we
1072 demonstrated that MIS19 and elevation structure these populations (RDA: P= 0.001, ANN:
1073 variable importance = 100).

1074

1075 *Hyrbid zone modeling in HZAR using snaplust and DAPC assignments:*

1076 We also fit clines for the same species pairs using individual genetic assignments: pure parental
1077 (0,1), backcross (0.25, 0.75), and F1 (0.5,0.5) and, alternatively, using adegenet prediction
1078 probabilities in the program HZAR v.2-9 (Derryberry et al. 2014). Using the Gaussian cline
1079 model, we estimated the center and width of the cline and determined if these sigmoidal
1080 distributions have significant tails by fitting the following models: 1) no tails, 2) right tail only,
1081 3) left tail only, 4) mirrored tails, and 5) both tails estimated independently (see Derryberry et al.
1082 2014). We fit these models to our data using AICc and ran the MCMC chains for $5x10^6$
1083 generations, thinned by $5x10^3$ generations, and estimated stationarity using ESS >200 in the R
1084 package CODA (Plummer et al. 2006).
1085 We found agreement for best-fit model between *spaclust* and DAPC assignments and
1086 parameter estimates. For the eastern lineages, HZAR showed strong support for a right-tailed
1087 model ($\Delta AIC_{snapclust}$ =-1.91 – -6.08, ΔAIC_{DAPC} =-31.96 – -107.42), whereas central lineages at
1088 the MR ($\Delta AIC_{snapclust}$ =-4.28 – -8.70, ΔAIC_{DAPC} = -4.26 – -8.869) and western lineages at the
1089 Desert and Edward's Plateau ($\Delta AIC_{snapclust}$ =-5.51 – -221.35, ΔAIC_{DAPC} = -5.51 – -221.35) both
1090 supported a no-tails model (Fig. 6; Table S4 & S5).
1091
1092
1093 *Genomics and the ICZN*
1094 Another problem likely to be encountered by other researchers using genomic data is that
1095 previously named type specimens at particular type localities may be from regions that show
1096 some admixture. For instance, the type locality of the eastern-most species, *P. alleghaniensis* is
1097 "the summit of the Blue Ridge in Virginia and the Highlands of the Hudson" (Holbrook 1836;
1098 Schultz 1996). Both areas are likely composed of admixed individuals and the International Code

of Zoological Nomenclature (ICZN) forbids naming species based on hybrids (Article 1.3.3;ICZN, 1999) though the intention of this ICZN article did not consider proportions of admixture. One possible solution would be to use the next available name from Florida, where no admixture is present (eliminating *P. quadrivittata*), which would be *P.deckerti* (type locality: Lower Matecumber Key, FL; Brady 1932). Another solution would be to designate a Neotype from a locality showing no admixture and retain *P. alleghaniensis.* If *P. alleghaniensis/P. spiloides* were not considered unique, then *P. alleghaniensis* has priority by 18 years (Holbrook 1836; Duméril et al. 1854).

The type locality for the remaining taxa, *P. spiloides (*New Orleans, Louisiana; Duméril et al. 1854), *P. obsoletus* (On the Missouri River from the Vicinity Isle au Vache to Council Bluff; Say, 1823), and *P. bairdi* (Fort Davis, Apache Mountains, Jeff Davis Co.: Texas; Yarrow 1880) are all from regions that likely represent individuals not admixed (Fig.1 & 5, Burbrink, 2001). Species delimitation methods, estimates of fixation for loci, and observation that these four organisms have remained geographically distinct in the face of gene flow throughout the Pleistocene suggests that these taxa should be considered unique species though hybrid zones exist. We acknowledge difficulties recognizing the eastern lineages as distinct and could argue for recognizing them as a single taxon, *P. alleghaniensis*.

Table S1. Priors and summary stats for PipeMaster for the IM, IMD, IMD-LGM models; estimating migration, timing of divergence, and historical demography.

IM

PARAMETER	**PRIOR.1**	**PRIOR.2**	**DISTRIBUTION**	
1	Ne0.pop1	20000	500000	runif
2	Ne0.pop2	20000	5e+05	runif
3	Ne0.pop3	20000	5e+05	runif
4	Ne0.pop4	20000	5e+05	runif
5	mig0.1_2	2	5	runif

6	mig0.1_3	0	0	runif
7	mig0.1_4	0	0	runif
8	mig0.2_1	2	5	runif
9	mig0.2_3	2	5	runif
10	mig0.2_4	0	0	runif
11	mig0.3_1	0	0	runif
12	mig0.3_2	2	5	runif
13	mig0.3_4	2	5	runif
14	mig0.4_1	0	0	runif
15	mig0.4_2	0	0	runif
16	mig0.4_3	2	5	runif
17	join1_2	30000	1000000	runif
18	join3_4	30000	1000000	runif
19	join2_4	500000	1700000	runif

IMD

PARAMETER	PRIOR.1	PRIOR.2	DISTRIBUTION	
1	Ne0.pop1	10000	500000	runif
2	Ne0.pop2	10000	500000	runif
3	Ne0.pop3	10000	500000	runif
4	Ne0.pop4	10000	500000	runif
5	mig0.1_2	2	5	rtnorm
6	mig0.1_3	0	0	rtnorm
7	mig0.1_4	0	0	rtnorm
8	mig0.2_1	2	5	rtnorm
9	mig0.2_3	2	5	rtnorm
10	mig0.2_4	0	0	rtnorm
11	mig0.3_1	0	0	rtnorm
12	mig0.3_2	2	5	rtnorm
13	mig0.3_4	2	5	rtnorm
14	mig0.4_1	0	0	rtnorm
15	mig0.4_2	0	0	rtnorm
16	mig0.4_3	2	5	rtnorm
17	Ne1.pop1	1000	10000	runif
18	Ne1.pop2	1000	10000	runif
19	Ne1.pop3	1000	10000	runif
20	Ne1.pop4	1000	10000	runif
21	t.Ne1.pop1	3000	170000	runif
22	t.Ne1.pop2	3000	170000	runif
23	t.Ne1.pop3	3000	170000	runif
24	t.Ne1.pop4	3000	170000	runif
25	join1_2	30000	1000000	runif
26	join3_4	30000	1000000	runif
27	join2_4	500000	1700000	runif

IMD-LGM

PARAMETER	PRIOR.1	PRIOR.2	DISTRIBUTION	
1	Ne0.pop1	10000	500000	runif
2	Ne0.pop2	10000	500000	runif
3	Ne0.pop3	10000	500000	runif
4	Ne0.pop4	10000	500000	runif
5	mig0.1_2	2	5	rtnorm
6	mig0.1_3	0	0	rtnorm
7	mig0.1_4	0	0	rtnorm
8	mig0.2_1	2	5	rtnorm
9	mig0.2_3	2	5	rtnorm
10	mig0.2_4	0	0	rtnorm
11	mig0.3_1	0	0	rtnorm
12	mig0.3_2	2	5	rtnorm
13	mig0.3_4	2	5	rtnorm
14	mig0.4_1	0	0	rtnorm
15	mig0.4_2	0	0	rtnorm
16	mig0.4_3	2	5	rtnorm
17	Ne1.pop1	1000	10000	runif
18	Ne1.pop2	1000	10000	runif
19	Ne1.pop3	1000	10000	runif
20	Ne1.pop4	1000	10000	runif
21	t.Ne1.pop1	3000	170000	runif
22	t.Ne1.pop2	3000	170000	runif
23	t.Ne1.pop3	3000	170000	runif
24	t.Ne1.pop4	3000	170000	runif
25	mig1.1_2	0	0	runif
26	mig1.1_3	0	0	runif
27	mig1.1_4	0	0	runif
28	mig1.2_1	0	0	runif
29	mig1.2_3	0	0	runif
30	mig1.2_4	0	0	runif
31	mig1.3_1	0	0	runif
32	mig1.3_2	0	0	runif
33	mig1.3_4	0	0	runif
34	mig1.4_1	0	0	runif
35	mig1.4_2	0	0	runif
36	mig1.4_3	0	0	runif
37	t.mig1.1_2	0	8700	runif
38	t.mig1.1_3	0	8700	runif
39	t.mig1.1_4	0	8700	runif
40	t.mig1.2_1	0	8700	runif
41	t.mig1.2_3	0	8700	runif
42	t.mig1.2_4	0	8700	runif
43	t.mig1.3_1	0	8700	runif
44	t.mig1.3_2	0	8700	runif
45	t.mig1.3_4	0	8700	runif

46	t.mig1.4_1	0	8700	runif
47	t.mig1.4_2	0	8700	runif
48	t.mig1.4_3	0	8700	runif
49	join1_2	30000	1000000	runif
50	join3_4	30000	1000000	runif
51	join2_4	500000	1700000	runif

Table S2 – PHRAPL Results. Available upon request (*open with R read.table() or Excel*).

Table S3. Results from RDA (F and P values) and ANN (variable importance [VAR_IMP]) for climate, distance, Mississippi River, and elevation variables . Significance of variables after variable inflation factors (VIF) are considered.

VARIABLES	RDA F VALUE	RDA P VALUE	P_VALUE_VIF	NN_VAR_IMP	NN_VAR_IMP_VIF
ALL TAXA					
MISSISSIPPI	14.1683	0.0001	0.001	100	100
MPW	1.3642	0.06	NA	31	NA
LGM	1.6455	0.015	NA	91	NA
LIG	1.4935	0.024	NA	6	NA
MIS	1.7603	0.005	0.001	81	100
CURRENT	1.8522	0.009	NA	0	NA
ELEVATION	0.9627	0.458	0.002	91	100
DISTANCE	Factored	Factored	Factored	100	100
EAST_OF THE_MS					
LGM	1.7148	0.001	0.001	70	100
LIG	2.0434	0.001	NA	100	NA
MIS	3.1272	0.001	NA	41	NA
CURRENT	1.8641	0.001	NA	98	NA
ELEVATION	1.0464	0.275	0.001	0	100
DISTANCE	Factored	Factored	Factored	100	100
WEST_OF_THE_MS					
LGM	1.4705	0.013	NA	72	NA
LIG	1.1802	0.192	NA	100	NA
MIS	0.9094	0.632	0.001	79	100
CURRENT	0.9583	0.533	NA	91	NA
ELEVATION	0.626	0.984	0.31	90	100
DISTANCE	Factored	Factored	Factored	100	100

Table S4. Results from cline modeling using HZAR for each species pair grouping using snapclust ancestry estimates

PANTHEROPHIS_ALLEGHANIENSIS_X_P.SPILOIDES

MODEL	Center	Width	Tail_Right	Tail_Left	Tail_Mirror	AICc	ESS
NONE	729 (723-735)	141 (127-157)	-	-	-	-65.158	717-5200
RIGHT	729 (723-736)	141 (126-157)	859 (375-1599)	-	-	-67.067	530-37423
LEFT	729 (723-735)	141 (126-157)	-	1143 (593-1679)	-	-60.988	829-53146
MIRROR	729 (723-735)	141 (126-157)			880 (251-1636)	-61.575	321-53591
BOTH	730 (724-736)	141 (126-157)	769 (147-1562)	1226 (719-1723)	-	-62.885	358-23637

PANTHEROPHIS_SPILOIDES_X_P.OBSOLETUS

MODEL	Center	Width	Tail_Right	Tail_Left	Tail_Mirror	AICc	ESS
NONE	801 (795-807)	100 (90-110)	-	-	-	-535.0162	14399-95534
RIGHT	801 (795-808)	100 (90-110)	1290 (721-1816)	-	-	-530.734	676-79146
LEFT	801 (795-808)	100 (90-110)	-	1276 (709-1835)	-	-530.735	20873-100521
MIRROR	801 (795-807)	100 (90-110)	-	-	1307 (762-1848)	-530.732	10695-120834
BOTH	802 (795-808)	99 (90-110)	1299 (770-1830)	885 (323-1638)	-	-526.3181	612-32572

PANTHEROPHIS_BAIRDI_P.OBSOLETUS

MODEL	Center	Width	Tail_Right	Tail_Left	Tail_Mirror	AICc	ESS
NONE	617 (575-670)	7 (3-13)	-	-	-	-150.277	5-1e5
RIGHT	617 (575-670)	10 (4-17)	1204 (613-1803)	-	-	-144.766	14-109080
LEFT	188 (635-2094)	70 (6-123)	-	647 (440-970)	-	71.072	3-523
MIRROR	642 (590-876)	12 (5-182)	-	-	757(37-1578)	58.219	1-915
BOTH	616 (574-660)	9 (4-16)	1218 (617-1810)	1198 (609-1810)	-	-138.23	9-98456

1152

1153 Table S5. Results from cline modeling using HZAR for each species pair grouping using
1154 adegenet ancestry estimates.
1155

PANTHEROPHIS_ALLEGHANIENSIS_X_P. SPILOIDES

MODEL	Center	Width	Tail_Right	Tail_Left	Tail_Mirror	AICc	ESS
NONE	938 (918-954)	552 (507-599)	-	-	-	62.806	1393-2686
RIGHT	753(747-760)	141 (126-157)	53 (45-61)	-	-	-44.61	970-3782
LEFT	912 (883-939)	610 (544-681)	-	188 (59-1433)	-	-60.988	129-514
MIRROR	760 (746-911)	155 (116-502)			91 (66-177)	64.53	6-350
BOTH	750 (740-757)	120 (64-136)	53 (47-60)	819 (278-1559)	-	-12.65	33-1717

PANTHEROPHIS_SPILOIDES_X_P.OBSOLETUS

MODEL	Center	Width	Tail_Right	Tail_Left	Tail_Mirror	AICc	ESS
NONE	797 (790-803)	97 (89-107)	-	-	-	-528.48	12066-16809
RIGHT	797 (790-803)	98 (88-107)	11335 (809-1857)	-	-	-524.22	363-29907
LEFT	797 (790-803)	98 (89-107)	-	1281 (718-1841)	-	-524.22	4278-36224
MIRROR	797 (790-803)	98 (89-107)	-	-	1302 (763-1851)	-524.22	3565-41252
BOTH	797 (791-804)	97 (88-106)	1327 (791-1864)	890 (235-1646)	-	-519.79	184-7761

PANTHEROPHIS_BAIRDI_P.OBSOLETUS

MODEL	Center	Width	Tail_Right	Tail_Left	Tail_Mirror	AICc	ESS
NONE	617 (575-660)	7 (4-13)	-	-	-	-150.277	10-34416
RIGHT	617 (575-661)	10 (5-20)	1204 (595-1793)	-	-	-144.766	6-24620
LEFT	652 (595-1874)	7 (3-81)	-	647 (465-1515)	-	71.072	7-400
MIRROR	617 (574-661)	11 (5-19)	-	-	1219(622-1807)	-144.76	9-38425
BOTH	617 (574-660)	8 (3-13)	1211 (619-1806)	1235 (635-1824)	-	-138.29	2-367770

1156
1157

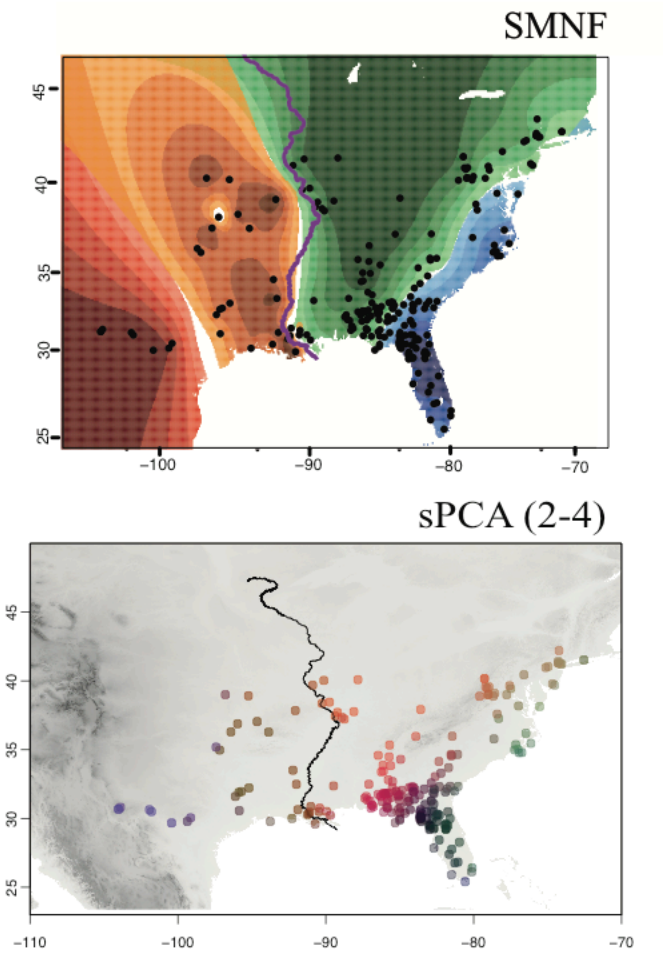

Fig.S1. Delimiting populations using sparse nonnegative matrix factorization (SNMF) and spatial Principal Component analysis (sPCA) showing the location of four geographically distinct lineages.

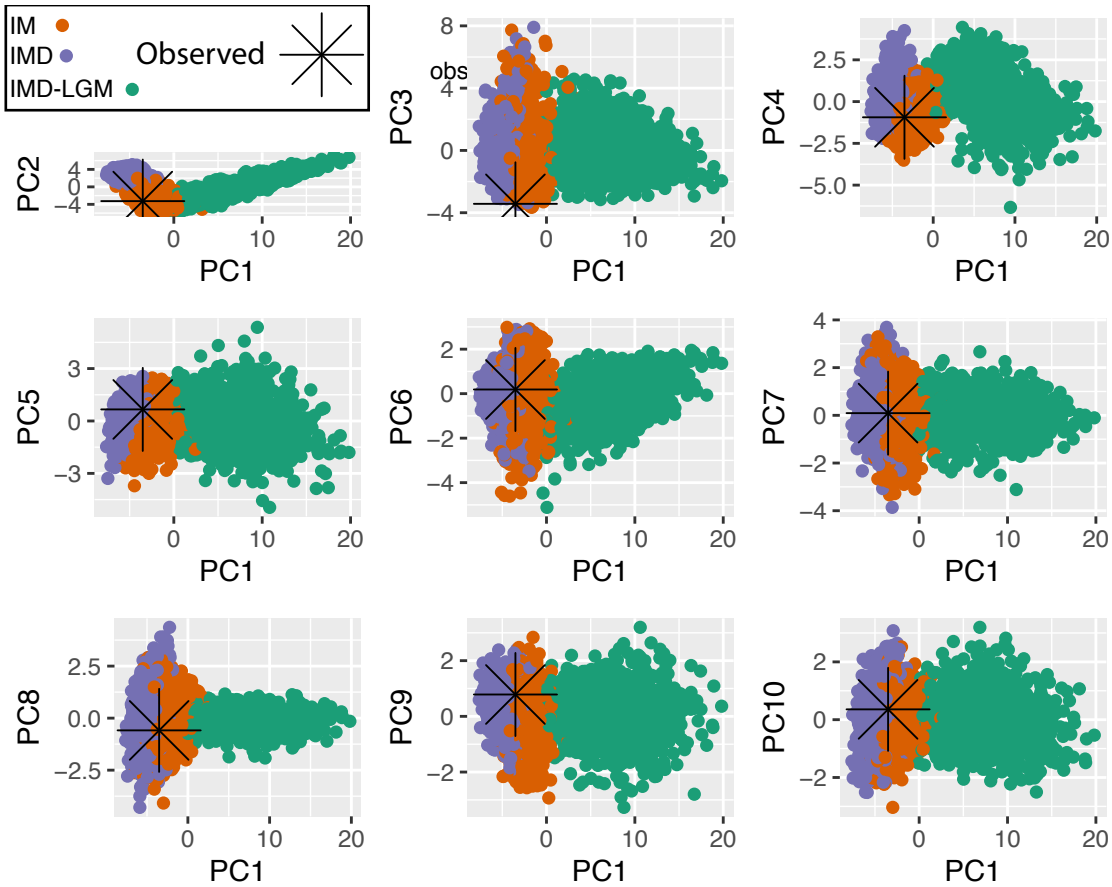

Fig. S2 – PipeMaster model fit of observed data to simulations under IM, IMD, and IMD-LGM models for PC1-PC10.

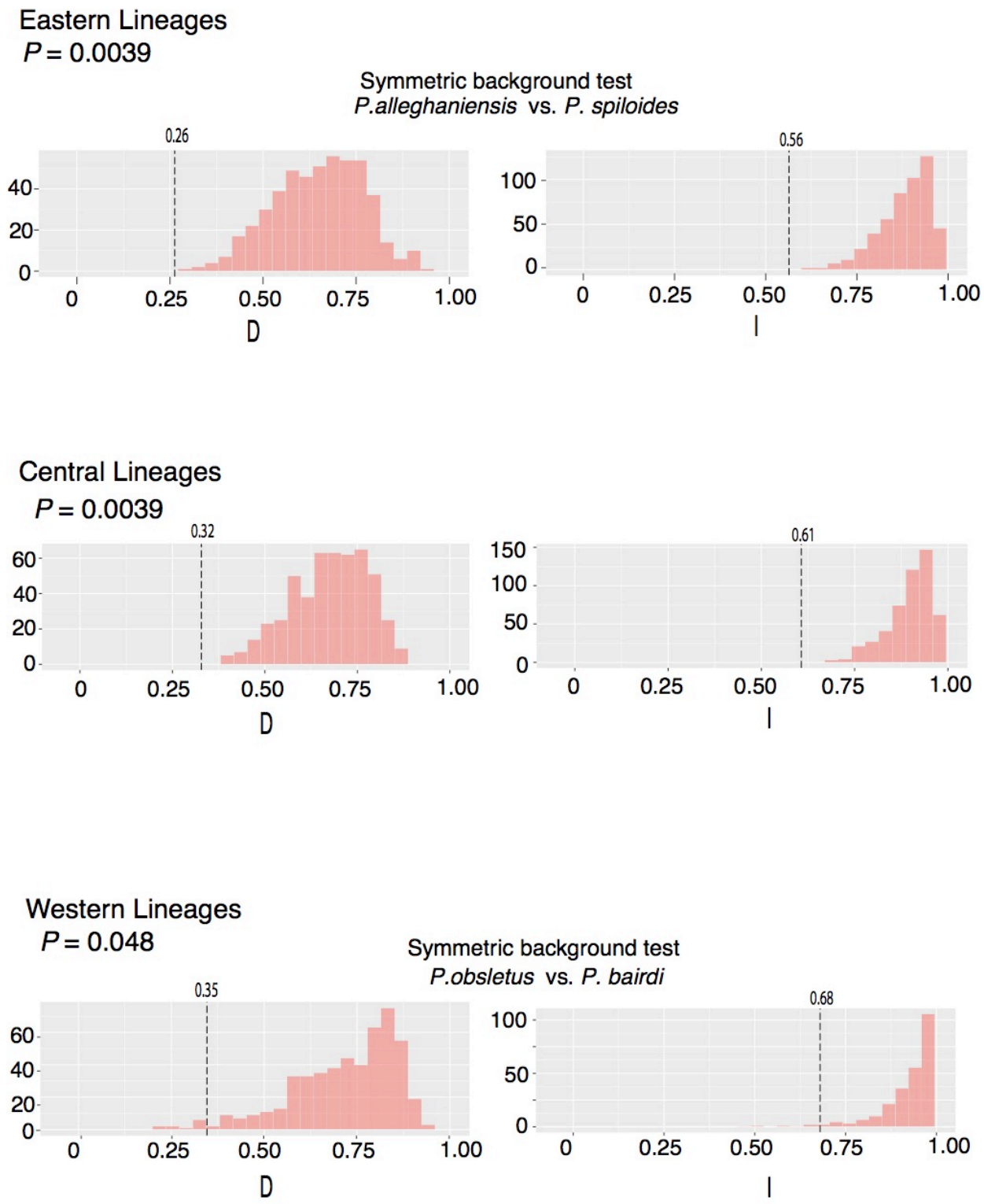

1203 Fig. S3 – Symmetric background niche similarity tests for spatially adjacent pairs (eastern,

1204 central, and western lineage comparisons) for the *D* and *I* statistics.

1205

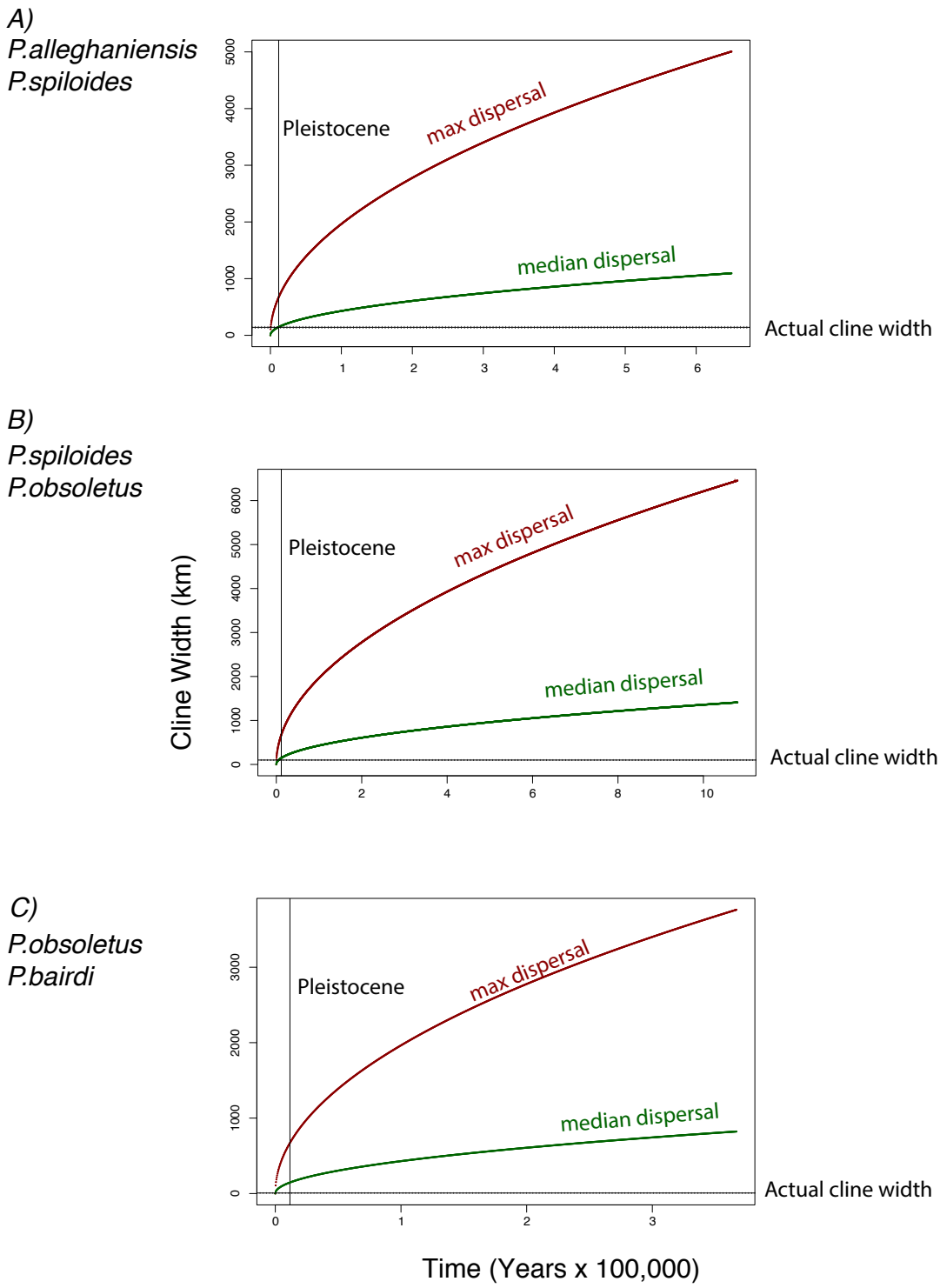

Fig. S4 – Prediction of cline width under neutrality given origin times for each species pair: A) *Pantherophis alleghaniensis/P. spiloides*, B) *P. spiloides/P.obsoletus*, and C) *P. obsoletus/P.bairdi.*

1209